Radiopharmaceuticals for Therapy 17

Hippocrates (ca. 460 BC–ca. 370 BC), a Greek physician (referred to as the Father of Medicine) described several kinds of cancer, referring to them by the term *karkinos (carcinos),* the Greek word for crab or crayfish, as well as carcinoma.

In the second century AD, the Greek physician Galen used *oncos* (Greek for swelling) to describe all tumours, reserving Hippocrates term *carcinos* for malignant tumours. Galen also used the suffix *-oma* to indicate cancerous lesions. It is from Galen's usage that we derive the modern word oncology. (WIKIPEDIA)

17.1 Introduction

Radiation therapy or radiotherapy is the medical use of ionizing radiation (high-energy electromagnetic waves or particles, such as X-rays, gamma rays, electron beams, or protons), generally as part of cancer treatments to control malignant cells. External beam radiation therapy (EBRT or XRT) or teletherapy, can be conducted using a γ beam from a radioactive cobalt-60 source, high-energy X-rays or electrons from linear accelerators (LINAC), and high-energy protons and neutrons from accelerators. In brachytherapy, a radioactive sealed source is put inside the body into or near the tumor. With some types of brachytherapy, Iridium-192 implants (wire or needles), or iodine-125 and palladium-103 seeds are used for treatment.

In systemic radiation therapy, also known as endoradiotherapy or radionuclide therapy (RNT), radioactive drugs (radiopharmaceuticals) given by mouth or injected directly into blood circulation (through a vein or an artery) are used to treat certain types of cancer. These radioactive drugs then travel throughout the body and deliver the radioactivity to both cancer cells and normal cells. Both teletherapy and brachytherapy play a key role in the treatment of cancer in a specific region in the body but, they are not useful for the treatment of widespread metastases.

Henri Becquerel received a skin burn from a vial of radium that he carried in his pocket. Pierre Curie performed experiments on his own skin to confirm this effect and suggested in 1903 that radium's ability to induce deep flesh burns might have potential in cancer therapy. Early attempts at radiation therapy utilized sources of radium salts to treat a variety of ailments including uterine cervical cancer, arthritis, skin lesions, lupus, and throat cancers [1]. In 1913, Frederick Proescher published the first study on the intravenous injection of radium for therapy of various diseases. Those early potential clinical uses have ended for health and safety concerns. However, the discovery of radium brought radioactivity to the attention of the general public and inspired many new uses of radioactivity.

In the 1920s, George de Hevesy, coined the term *radioindicator* or *radiotracer* and introduced the *tracer principle* in biomedical sciences. Also in 1920s, the first tracer study in rabbits was performed to investigate the absorp-

S. Vallabhajosula, *Molecular Imaging and Targeted Therapy*,
https://doi.org/10.1007/978-3-031-23205-3_17

tion, circulation and excretion of labeled bismuth preparations containing Radium E (identified later as ^{210}Bi, a beta emitter with a half-life of 5 days) [2]. The study showed that bismuth hydroxide suspended in oil was most suitable for therapeutic application of syphilis [3]. Also, Chieivitz and Hevesy administered P-32 phosphate to rats and demonstrated the renewal of the mineral constituents of bone.

In 1936, John H. Lawrence, the brother of Ernest Lawrence, made the first clinical therapeutic application of an artificial radionuclide when he used phosphorus-32 to treat leukemia. In 1941, Saul Hertz gave a patient the first therapeutic dose of iodine-130 (a β^- emitter with a half-life of 12.36 h). However, the discovery of ^{131}I by Glenn Seaborg and John Livingood at the University of California, Berkeley, has been the success story in nuclear medicine. In 1946, the first patient received [^{131}I]iodide, the "atomic cocktail" for the treatment of thyroid cancer [4]. I-131 has the advantage of emitting both γ rays and β^- rays, the former enabling imaging for diagnosis and dosimetry and the latter being valuable for molecular radiotherapy of hyperthyroidism and thyroid cancer. [^{131}I]sodium iodide was the first radiopharmaceutical to receive regulatory approval for routine clinical use in patients with thyroid disease.

17.2 Radiopharmaceuticals

A radiotracer can be defined as a specific radiolabeled molecule that resembles or traces the in vivo behavior of a natural molecule and can be used to provide information about a specific biological process. A radioligand can be defined as any radiolabeled molecule that can bind with another molecule or substance (binder) in a predictable way under controlled conditions. All radiolabeled compounds or substances used for the purpose of diagnosis or therapy have been defined as radioactive drugs or radiopharmaceuticals by the U.S. Food and Drug Administration (FDA).

The term *unconjugated* radiopharmaceutical has been generally defined as referring to those radionuclides that target specific disease sites by virtue of chemical, biologic, or physical affinity of radioisotope itself, rather than by virtue of carrier agents to which they are tagged. Because of the untagged nature of their use, *unconjugated* radiopharmaceuticals are also referred as *naked* radiopharmaceuticals. During the last couple of decades, there has been significant increase in the application of *conjugated* radiopharmaceuticals for targeted radionuclide therapy (TRT), mainly due to the development of a range of new carrier molecules (targeting vehicle), which can transport the radionuclide to a molecular target on the cancer cell (Fig. 17.1). The key factors that influence tumor localization of *conjugated* radiopharmaceuticals include the chemical and biochemical nature of the carrier molecule transporting the radionuclide of choice to the targeted area [5].

A century ago, Paul Ehrlich postulated the notion that a *magic bullet* could be developed to selectively target the disease and speculated that antibodies could function as magic bullets. The first demonstration of TRT was the use of ^{131}I-labeled polyclonal antibodies for the treatment of patients with melanoma. Several *unconjugated* or *conjugated* radiopharmaceuticals are now available commercially for the treatment of different benign diseases and malignancies (Table 17.1). In addition, some of the important new therapy radiopharmaceuticals under clinical investigation are summarized in Table 17.2. Several review articles and book chapters have extensively discussed the development of targeted radiopharmaceuticals for therapy [5–7].

17.2.1 Therapy Radiopharmaceuticals

Radiopharmaceutical therapy (RPT) or Targeted Radionuclide therapy (TRT) is defined by the delivery of radioactive atoms to tumor tissue or tumor-associated targets. Therapeutic radiopharmaceuticals may be structurally simple ions (^{131}I, $^{89}Sr^{2+}$, and $^{223}Ra^{2+}$), small molecules (^{131}I-MIBG and ^{153}Sm-EDTMP), complex molecules (^{131}I, ^{90}Y, or ^{177}Lu-labeled intact antibodies or antibody fragments), colloids (^{32}P chromic phosphate), or even particles (^{90}Y-labeled microspheres). The

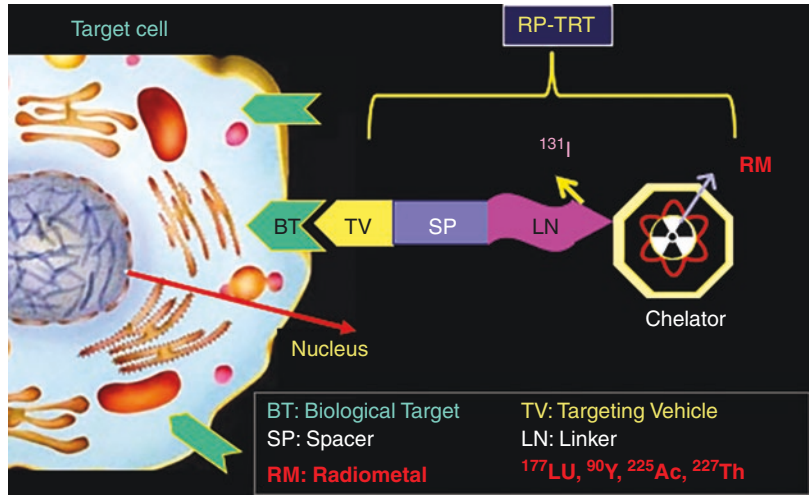

Fig. 17.1 Schematic of a conjugated radiopharmaceutical for targeted radionuclide therapy (TRT)

Table 17.1 FDA-approved radiopharmaceuticals for therapy

Radiopharmaceutical	Trade name	Decay	Target	Indication
[^{32}P]Sodium orthophosphate		β^-	Against primary cancers as well as distant metastases	Polycythemia vera
[^{131}I]Sodium iodide		β^-	Active transport via NaI symporter	Hyperthyroidism
				Thyroid cancer
[^{89}Sr]Strontium chloride	Metastron®	β^-	Bone hydroxyapatite	Palliative therapy of pain due to bone metastasis
[^{153}Sm]Lexidronam (EDTMP)	Quadramet®	β^-	Bone hydroxyapatite	Palliative therapy of pain due to bone metastasis
[^{223}Ra]Radium dichloride	Xofigo®	α	Bone hydroxyapatite	Metastatic prostate cancer
^{90}Y-labeled glass microspheres	Theraspheres®	β^-	Embolization of hepatic arterioles	Hepatic malignancy
^{90}Y-labeled resin microspheres	Sir Spheres®	β^-	Embolization of hepatic arterioles	Hepatic malignancy
^{131}I-Tositumomab	Bexxar®	β^-	CD-20 on B cells	Non-Hodgkin's follicular lymphoma
^{90}Y-Ibritumomab tiuxetan	Zevalin®	β^-	CD-20 on B cells	Non-Hodgkin's follicular lymphoma
[^{131}I]Iobenguane, MIBG	AZEDRA®	β^-	Norepinephrine transporter	Pheochromocytoma
				Paraganglioma. NETs
^{177}Lu-DOTATATE	LUTATHERA®	β^-	Somatostatin type II receptor (SSTR-II)	Neuroendocrine tumors
^{177}Lu-PSMA-617	Pluvicto	β^-	Prostate-specific membrane antigen (PSMA)	Metastatic castration-resistant prostate cancer (mCRPC)

tumor localization properties of a specific therapeutic radiopharmaceutical and the clinical application will depend on the route of administration, such as oral, intravenous, intra-arterial, intracavitary, and intra-articular approaches. The ideal physical and biological properties of a radiopharmaceutical intended for therapy should be such that a large, absorbed radiation dose is deposited in the tumor, or diseased tissue, with minimal radiation dose to the normal tissues. This requires the use of an appropriate radionuclide, administered in a suitable chemical form with optimal

Table 17.2 Therapy radiopharmaceutical under clinical investigation

Radiopharmaceutical		Decay	Target	Indication	Clinical trial
^{131}I-Apamistamab (IOMAB-B)	Actinium Pharmaceuticals	β^-	BC8 mAb targeting CD-45	Bone marrow ablation in AML	Phase III SIERRA trial
^{225}Ac-Lintuzumab (Actimab-A)	Actinium Pharmaceuticals	α	M195 mAb Targeting CD-33	Bone marrow ablation in AML	Phase I and II
^{177}Lu-huJ591 mAb	Weill Cornell Medicine	β^-	PSMA	CRMPC	Phase II
^{225}Ac-huJ591 mAb	Weill Cornell Medicine	α	PSMA	CRMPC	Phase I, II
^{177}Lu- DOTA-JR11	IPSEN	β^-	SSTR mediated	NETs	Phase I, II
^{177}Lu-PSMA-R2	Novartis/AAA	β^-	PSMA	Prostate cancer	Phase II
^{177}Lu-DOTA-N3-CTT1403	NCI	β^-	PSMA	Prostate cancer	Phase I/II
^{227}Th-MSLN-TTCa	Bayer	α	Mesothelin		Phase I
^{227}Th-PSMA-TTCa	Bayer	α	PSMA	Prostate cancer	Phase I
^{227}Th-CD22-TTC	Bayer	α	CD22 B-cell	Lymphoma	Phase I
^{225}Ac- FPX-01a	J&J Fusion Pharma	α	Insulin growth factor 1	NSC lung cancer	Phase I
^{225}Ac-PSMA-617	Endocyte/Novartis	A			

specific activity (mCi or MBq/mmol), and by an appropriate route of administration, which will allow selective uptake in the target tissue in sufficient concentration to elicit a therapeutic response. Different mechanisms, however, are involved in the delivery and accumulation of the therapeutic agent within the tumor cells. However, the remarkable potential of RPT directed against primary cancers as well as distant metastases, is now recognized as an effective and safe and treatment modality.

17.3 Radionuclides for Therapy

Although numerous radionuclides have potential applications in radionuclide therapy, only a very few radionuclides possess favorable nuclear, physical, chemical, and biological characteristics which would identify them as practical for clinical use. Some of the important radionuclides used in the development of therapeutic radiopharmaceuticals are listed in Table 17.3. The ideal radionuclides for therapy are those with an abundance of non-penetrating radiations, such as charged particles (α^{2+}, β^-, *and Auger electrons*) and lack of penetrating radiations (γ or X-rays). While penetrating radiation is not essential for TRT, a small amount or abundance with an appropriate energy (100–400 KeV) may be useful for imaging studies to demonstrate tumor localization or altered biodistribution.

17.3.1 Radionuclides-Emitting Beta Particles

The physical characteristics of β^- emitting radionuclides are summarized in Table 17.4. In beta decay, fast energetic electron (β^-) or positron (β^+) is emitted from an atomic nucleus, transforming the original nuclide to an isobar of that nuclide. In neutron-rich nuclides, a neutron transforms it into a proton by the emission of an electron and an antineutrino. The fast energetic electrons are called beta (β^-) particles. In neutron-deficient nuclides, a proton is converted into a neutron by the emission of a positron (β^+) and a neutrino. Most of the radionuclides in routine clinical use are β^- emitters (^{131}I, ^{90}Y, ^{177}Lu, ^{89}Sr, and ^{153}Sm) with a wide range of half-lives ranging from 1.95 to 59.5 days Table 17.4. The kinetic energy spectrum of β^- particles consist of a continuum of energies ranging from almost zero to their maxi-

Table 17.3 Production methods of radionuclides used for therapy

Radionuclide	$T_{½}$ (days)	Decay	Production method (nuclear reaction)
^{32}P	14.268	β⁻	^{31}P(n, γ)^{32}P
			^{32}S(n, p)^{32}P
^{89}Sr	50.53	β⁻	^{88}Sr(n, γ)^{89}Sr, ^{89}Y(n, p)^{89}Sr
^{169}Er	9.4	β⁻	^{168}Er(n, γ)^{169}Er
^{131}I	8.02	β⁻, γ	^{235}U(n, fission)^{131}I
			^{130}Te(n, γ)^{131}Te $\rightarrow_{\beta^-}$ ^{131}I
^{161}Tb	6.90	β⁻, γ	^{160}Gd(n, γ) ^{161}Gd → ^{161}Tb
^{177}Lu	6.73	β⁻, γ	^{176}Lu(n, γ)^{177}Lu
			^{176}Yb(n, γ)^{177}Yb $\rightarrow_{\beta^-}$ ^{177}Lu
^{186}Re	3.777	β⁻	^{185}Re(n, γ)^{186}Re
^{198}Au	2.697	β⁻	^{197}Au(n, γ)^{198}Au
^{90}Y	2.67	β⁻	^{235}U(n, fission)^{90}Sr $\rightarrow_{\beta^-}$ ^{90}Y
			^{90}Sr $\rightarrow$ ^{90}Y0 Generator
^{67}Cu	2.58	β⁻	^{67}Zn(n, p)^{67}Cu
^{153}Sm	1.9375	β⁻	^{152}Sm(n, γ)^{153}Sm
^{77}As	1.60	β⁻	^{nat}Ge(n, γ)77Ge $\rightarrow_{\beta^-}$ ^{77}As
^{166}Ho	1.120	β⁻	^{165}Ho(n, γ)^{166}Ho
^{188}Re	0.708	β⁻	^{187}W(n, γ)^{188}W $\rightarrow_{\beta^-}$ ^{188}Re
			^{188}W → ^{188}Re Generator
^{117m}Sn	0.566	IT, CE	^{116}Sn(n, γ)^{117m}Sn
			^{117}Sn (n, n′, γ) ^{117m}Sn
^{212}Pb $\rightarrow$ ^{212}Bi[a]	0.442	β⁻	^{228}Th $\rightarrow$ ^{224}Ra $\rightarrow$ ^{212}Pb $\rightarrow$ ^{212}Bi *g*enerator
		α (from ^{212}Bi)	
^{213}Bi[a]	45.6 m	A	^{225}Ac $\rightarrow$ ^{213}Bi generator
^{211}At	7.2 h	A	^{209}Bi(α, 2n)^{211} (accelerator produced)
^{149}Tr	4.12 h	α, and β⁺	^{nat}Nd(^{12}C,xn)^{149}Dy $\rightarrow$ ^{149}Tb (cyclotron produced)
^{225}Ac[a]	10.0	A	^{229}Th $\rightarrow$ ^{225}Ac generator
			^{232}Th(p, x)^{225}Ac (accelerator produced)
^{223}Ra[a]	11.43	A	^{227}Ac $\rightarrow$ ^{227}Th $\rightarrow$ ^{223}Ra generator
^{227}Th[a]	18.7	α, and β⁺	^{227}Ac $\rightarrow$ ^{227}Th generator

[a] The alpha emitters are regarded as in vivo generators because following administration into a patient, they generate alpha-emitting daughters

mum energy (E_{max}), and the average energy (E_{avg}) of a β⁻ particle is about one-third of the maximum energy (Fig. 17.2a). The average range of electrons in tissue can be between 0.1 and 5.0 mm depending on the kinetic energy. As a result, beta particles can pass through several cells (10–1000), a useful property that has been termed "crossfire effect," which ensures sufficient dose delivery to each cell in a large tissue mass. The beta particle-emitting radionuclides can be arranged into three groups according to the mean range in tissue: short range (<1 mm), medium range (1–2 mm), and long range (>2 mm). It is important to match the range of the radionuclide with the anticipated size of the tumor target. Small tumors were more effectively treated by a short-range b emitter, while a higher cure rate could be obtained in larger tumors with a long-range b emitter [8].

17.3.1.1 Phosphorous-32

^{32}P ($T_{½}$ = 14.268 days) decays into ^{32}S by the emission of β⁻ (E_{max} = 1.709 MeV) particles. ^{32}P has been available for the treatment of myeloproliferative neoplasms for over 80 years. ^{32}P can be produced in a reactor by neutron activation using ^{31}P(n, γ)^{32}P reaction. However, the specific activity of ^{32}P is very low since the product can't be

Table 17.4 Physical characteristics of beta-emitting radionuclides for targeted therapy

	*T*½ (days)	β⁻ particle energy (MeV)		β⁻ particle range in soft tissue (mm)		Energy of γ photons	
Radionuclide	Days	Max	Average	Max	Mean	KeV	%
^{199}Au	3.14	0.452	0.082		0.41	158	36.9
						494	97
^{169}Er	9.4	0.351	0.101		0.51	110	0.0014
^{177}Lu	6.73	0.497	0.133	1.8	0.67	113	6.6
						208	11
^{67}Cu	2.58	0.60	0.141		0.71	93.3	16
						184.6	47
^{161}Tb	6.9	0.593	0.154		0.77	74	9.8
						49	14.8
^{47}Sc	3.4	0.600	0.162		0.81	159	68
^{131}I	8.02	0.606	0.182		0.91	364	81
^{77}As	1.60	0.700	0.228		1.20	239	1.60
^{153}Sm	1.9375	0.808	0.229		1.20	70	5.25
						103	28.3
^{198}Au	2.697	0.960	0.315	3.6	1.60	411	95.6
^{186}Re	3.777	1.077	0.362	3.6	1.80	137	8.6
^{89}Sr	50.53	1.496	0.58	8.0	2.5	910	1
^{166}Ho	1.120	1.850	0.666	8.1	3.2	80.6	6.6
^{32}P	14.27	1.710	0.695	7.9	2.9	–	–
^{188}Re	0.708	2.12	0.764		3.5	188	15
^{90}Y	2.67	2.28	0.935	12	3.9	–	–
^{198}Au	2.697	0.96	99	3.6		411	95.6
^{90}Y	2.67	2.28	100	12.0	3.6		
^{117m}Sn	13.60	0.13	64.9	0.22		159	86.4
		0.15	26.2	0.29			

separated from the target by traditional methods. However, the ^{32}S(n, p)^{32}P nuclear reaction is ideal since the target and the product are two different elements. ^{32}P can be easily separated and purified from the target and is usually carried out following wet chemical extraction and dry distillation methods and supplied in high specific activity but, the contribution of the longer-lived ^{33}P (*T*½ 25.3 days) is of concern as a radionuclidic impurity. ^{32}P is supplied as orthophosphoric acid in water with a specific activity of 8–9 Ci (314–337 TBq)/mmol.

17.3.1.2 Iodine-131

^{131}I ($T_{½}$ 8.02 days) decays by the emission of β⁻ (E_{max} = 606 KeV) particles and γ (364 KeV) emissions to stable ^{131}Xe inert gas. ^{131}I sodium iodide solution has been used for the management of thyroid disorder for almost 80 years. As a halogen, it can be easily incorporated into organic molecules, peptides, and antibodies. [^{131}I] MIBG (*m*-iodobenzylguanidine) is widely used for the treatment of neuroendocrine tumors. ^{131}I-Tositumomab (anti CD20 antibody, Bexaar®) is used for the treatment of non-Hodgkin's lymphoma.

^{131}I is a major fission product of ^{235}U and ^{239}Pu. comprising nearly 2.8336% of the total products of fission (by weight). Radionuclidic purity of fission produced ^{131}I is ≥99.9% of the total radioactivity. The specific activity is approximately 130 Ci/mg or 4.81 TBq/mg. A more practical method of ^{131}I production is based on (n, γ) reaction in a research reactor using ^{130}Te target, which is approximately 30% of natural tellurium element. Certain (n, γ) reactions produce a short-lived radioisotope of the target element, which decays by beta emission to another unstable radioactive nuclide with longer half-life compared to that of the intermediate. As shown below,

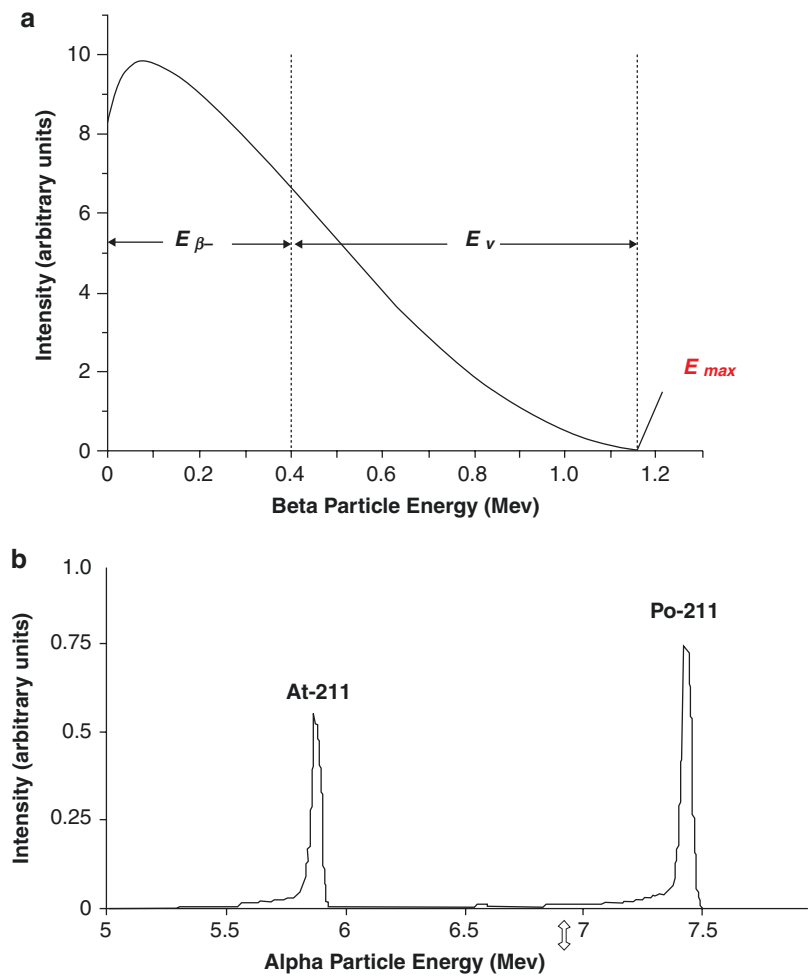

Fig. 17.2 (**a**, **b**) Energy spectrum

both the ground state ^{131}Te and metastable ^{131m}Te decay to ^{131}I.

$$^{130}Te\left(n,\gamma\right)^{131m}Te_{(33.25h)\rightarrow\beta^-}{}^{131}I \quad (17.1)$$

$$^{130}Te\left(n,\gamma\right)^{131}Te_{(25m)\rightarrow\beta^-}{}^{131}I \quad (17.2)$$

Following neutron irradiation, ^{131}I is extracted from the natural tellurium target generally by the dry distillation method. The process involves heating the irradiated sample to release the ^{131}I and ^{131}I in a sodium hydroxide solution (pH 8–10). Use of natural tellurium target also results in the production of stable ^{127}I and long-lived ^{129}I as chemical and radionuclidic impurities. As a result, the specific activity is generally less than that of fission-produced ^{131}I (4–5 TBq/mg).

17.3.1.3 Yttrium-90

^{90}Y ($T_{½}$ 64.1 h) is a pure β⁻ emitter and decays to stable zinc-90 with very high energy (E_{max} =2.28 MeV) and no γ emissions. As a trivalent metal, yttrium exhibits relatively simple ion chemistry forming complexes with a variety of chelating agents. Selective internal radiation therapy (SIRT) with ^{90}Y-labeled microspheres has become a widely employed brachytherapy for the treatment of primary and metastatic hepatic malignancies. ^{90}Y-ibritumomab tiuxetan (Zevalin®) is used for the treatment of NHL.

^{90}Y can be produced in a reactor by neutron irradiation of stable yttrium-89 via ^{89}Y(n, γ)^{90}Y reaction [9]. Exposing a 1 cm cube (approximately 5 g), natural yttrium target to 10^{14} n/cm^2/s flux would create Y-90 at a rate of 1.1 Ci/h. To make

high specific activity ^{90}Y, e-LINAC is used to generate a neutron beam (12.1 MeV) and directing the neutron beam onto the zirconium target (^{90}Zr) to isotopically convert some of the atoms to ^{90}Y via ^{90}Zr(n, p)^{90}Y. However, the most common method of producing high specific activity ^{90}Y is by the decay of the parent isotope ^{90}Sr ($T½$ = 29 years), which is a fission product of uranium. ^{90}Sr → ^{90}Y generator has been in clinical use for the last 4 decades [10]. The theoretical specific activity is 20 GBq (540 mCi)/μg of Yttrium-90.

17.3.1.4 Lutetium-177

^{177}Lu ($T_{½}$ 6.734 days) is a low-energy β⁻ emitter (E_{max} = 0.498 MeV) with suitable γ photons (113 and 208 KeV) suitable for SPECT imaging studies. ^{177}Lu-DOTATATE (Lutathera®) is the first ^{177}Lu peptide radiopharmaceutical approved by the FDA for TRT of patients with neuroendocrine tumors (NETs). Like other trivalent metals, ^{177}Lu forms strong complexes with bifunctional chelating agents. Several ^{177}Lu-labeled peptides and antibodies are in Phase II–III clinical trials for TRT.

^{177}Lu can be produced in a reactor by direct neutron activation via ^{176}Lu(n, γ)^{177}Lu reaction using enriched ^{176}Lu target. The direct production route also results in formation of a small amount of long-lived metastable ^{177m}Lu ($T_{½}$ 160 days) in activity (<0.02%). The specific activity depends on the ^{176}Lu enrichment and one can obtain 20–40 Ci/mg with >80% enriched ^{176}Lu targets. The amount of ^{177}Lu produced, however, depends on the neutron energy, neutron flux, and the irradiation time [11]. Using natural lutetium targets and high neutron flux reactors, it is possible to increase the yields and specific activity.

In the indirect route of neutron activation method, isotopically enriched ^{176}Yb target undergoes (n, γ) transmutation to produce ^{177}Yb which subsequently decays by β⁻ emission ($T_{½}$ 1.9 h) to yield ^{177}Lu. The major advantage of the indirect method is the production of no carrier added (NCA) ^{177}Lu which is then separated by suitable radiochemical processes. In addition, the indirect method does not produce any ^{177m}Lu radionuclide impurity. With enriched ^{176}Yb targets, it is possible to achieve very high specific activity approaching the theoretical specific activity of 110 Ci (4.07 TBq)/mg [11].

17.3.1.5 Copper-67

^{67}Cu ($T_{½}$ 2.58 days) a transition metal, decays by the emission of low-energy β⁻ particles (E_{max} = 0.562 MeV) and provides several γ photons (91, 93, 184 KeV) suitable for SPECT. The production of ^{67}Cu has been tested both in reactors and cyclotrons on a variety of nuclear reactions, such as ^{67}Zn(n,p)^{67}Cu, ^{68}Zn(p, 2p)^{67}Cu, and ^{70}Zn(p, α)^{67}Cu. The ^{68}Zn(p,2p)^{67}Cu route of production (using 70 MeV proton) appears to be the most attractive method. However, large quantities of ^{64}Cu ($T_{½}$ = 12.7 h) and ^{67}Ga ($T_{½}$ = 78.3 h) are the major radionuclidic impurities. The specific activity of ^{67}Cu is <20 mCi/μg [12].

A breakthrough in the production of high specific activity ^{67}Cu is based on the photonuclear activation, using highly enriched (98.9%) ^{68}Zn targets. For the ^{68}Zn(γ,p)^{67}Cu reaction, high-energy γ rays can be produced by bremsstrahlung conversion of electrons from e-LINAC [12, 13]. The specific activity of ^{67}Cu so produced has reached over 5.55 GBq/μg (150 mCi/μg). Due to this technical breakthrough in ^{67}Cu production, no-carrier-added ^{67}Cu has been made available in large scales at the US-DOE National Isotope Development Center.

17.3.1.6 Scandium-47

^{47}Sc ($T_{½}$ 3.35 days) with low-energy β⁻ particles (E_{max} = 441 keV) is ideal for therapy. In addition, the emission of 159 KeV γ photons is appropriate for SPECT imaging studies. Also, the positron emitters ^{43}Sc ($T_{½}$ = 3.89 h, $E_{β+avg}$ = 476 keV, I = 88.1%) and ^{44}Sc ($T_{1/2}$ 3.97 h, $E_{β+avg}$ = 632 keV, I = 94.3%) have been proposed for PET imaging studies. Like lutetium and yttrium, scandium also is a trivalent metal and has favorable chemistry for chelation and attachment to various molecular targeting agents.

^{47}Sc can be produced by two different neutron-induced reactions: ^{46}Ca(n, γ)^{47}Ca → ^{47}Sc or ^{47}Ti(n, p)^{47}Sc. The (n, γ) reaction is induced by thermal neutrons, while the (n, p) reaction requires fast neutrons (>1 MeV). Enriched ^{46}Ca as $CaCO_3$ is generally used for thermal neutron activation reaction. The chemical separation of Sc from Ca is performed using DGA resin and SCX cation exchange cartridges.

^{47}Sc can be produced with higher specific activities via the ^{48}Ti(γ, p)^{47}Sc photo nuclear reaction by irradiation of a natural titanium target [14–16]. Target foils dissolved in 2.0 M H_2SO_4. ^{47}Sc ions can be separated from natural titanium using AG MP-50 cation exchange resin. The recovered ^{47}Sc is purified using Chelex 100 ion exchange resin.

17.3.1.7 Terbium-161

^{161}Tb ($T_{1/2}$ 6.9 days) emits low-energy β^- particles [E_{max} = 593 keV) and also γ photons (74 and 49 KeV), and is useful for imaging studies. In addition, ^{161}Tb also emits a significant amount of conversion and Auger electrons. Greater therapeutic effect can therefore be expected in comparison to ^{177}Lu [17]. It also emits low-energy photons that are useful for gamma camera imaging. The trivalent cation chemistry of terbium is similar to lutetium and is, therefore, compatible with existing radiolabeling techniques to develop ^{161}Tb-labeled radiopharmaceuticals for TRT.

^{161}Tb can be reactor-produced by double-neutron capture on natural terbium by the ^{159}Tb(2n, 2γ)^{161}Tb reaction. However, the specific activity is low and not optimal for TRT. The alternative reactor production route is via the ^{160}Gd(n, γ)^{161}Gd ($T_{½}$ 3.66 m), which quickly decays by β^- emission to ^{161}Tb. To prevent the formation of several radionuclidic impurities it is important to use highly enriched ^{160}Gd targets. The specific activities of ~100 mCi/mg can be obtained using this method [18].

17.3.1.8 Strontium-90

^{89}Sr ($T_{½}$ = 50.53 days) is an alkaline earth metal and undergoes β^- decay (E_{max} = 1.495 MeV) into ^{89}Y with no gamma emissions. ^{89}Sr chloride (Metastron™) is used for bone pain palliation. ^{89}Sr is anthropogenic radionuclide that is a fission product with yields of 4.69 ± 0.06% [19].

^{89}Sr can also be produced by neutron activation using ^{88}Sr(n, γ)^{89}Sr using $SrCO_3$ as the target with thermal neutrons. A highly enriched target ^{88}Sr (>99%) is used to eliminate strontium-85 impurity. This is a convenient production method and takes place in a normal research reactor. ^{89}Sr can also be produced via ^{89}Y(n, p)^{89}Sr nuclear reaction using fast neutrons and yttrium oxide pellets.

17.3.1.9 Samarium-153

^{153}Sm($T_{½}$ = 1.93 days) is a transition metal and one of the elements in the lanthanide series. It decays by β^- emission (E_{max} = 0.810 MeV) to europium-153, with useful γ emissions (103 KeV). ^{153}Sm-EDTMP or Lexidronam (Quadramet®) is clinically used for bone pain palliation. ^{53}Sm is produced by neutron activation of both natural Sm_2O_3 and 98% enriched $^{152}Sm_2O_3$ targets via ^{152}Sm(n, γ)^{153}Sm nuclear reaction (IAEA-TECDOC-1340). Specific activity achieved at EOB is 14.8–16.8 GBq (400–450 mCi)/mg oxide. The specific activity of enriched ^{152}Sm targets can be up to 1200 mCi/mg.

17.3.1.10 Tin-117m

^{117m}Sn ($T_{½}$ 13.6 days) is a post-transition metal and decays by isomeric transition (*IT*) and emits low, and mono-energetic conversion electrons (0.127, 0.129, and 0.152 MeV). It also emits γ photons (159 KeV) suitable for SPECT. Bone marrow toxicity of this radionuclide is low because of its short-range (~3 mm) electrons. It is a novel radionuclide with low-energy electrons for radionuclide therapy applications, including rheumatoid arthritis and bone pain palliation, ^{117m}Sn can be produced in massive quantities as a low specific activity (up to 21 mCi/mg) product in reactors via the ^{116}Sn(n, γ)^{117m}Sn or ^{117}Sn(n,n′γ)^{117m}Sn reactions. A carrier-free, high specific activity (up to 20 Ci/mg) isotope can be manufactured with >50 MeV cyclotrons employing either stable antimony target ^{nat}Sb(p, x)^{117m}Sn or ^{116}Cd(α, 3n) nuclear reactions [20].

17.3.1.11 Re-186 and Re-188

^{186}Re ($T_{½}$ = 3.718 days) is a transition metal and decays by β^- emission (E_{max} = 1.07 MeV) with useful γ photons (137 KeV) for SPECT. ^{188}Re ($T_{½}$ = 16.9 h) also decays by β^- emission (E_{max} = 2.12 MeV) with useful γ photons (155 KeV) for SPECT. Since rhenium and technetium exhibit similar chemical properties, the preparation and targeting of $^{186/188}$Re radiophar-

maceuticals for therapy is similar to the preparation of ^{99m}Tc agents.

The primary production of ^{186}Re in a reactor is via ^{185}Re(n, γ)^{186}Re nuclear reaction using enriched ^{185}Re target (>94%). The typical specific activity is 1.84 Ci/mg [21]. High specific activity ^{186}Re can be produced using cyclotron irradiation of enriched tungsten-186 target via the ^{186}W(d, 2n)^{186}Re nuclear reaction. However, the target thickness and beam currents are critical to achieving high specific activity. Specific activity of 80 Ci/mg was obtained using a graphite-encased ^{186}W target and 18.7 MeV deuteron bombardment for 2 h, at a beam current of 27 μA [22].

^{188}Re as a no-carrier-added nuclide can be produced in high specific activity from the ^{188}W → ^{188}Re generator system. ^{188}W ($T_{½}$ 69.78 days) decay by β⁻ emission to ^{188}Re. The parent ^{188}W is produced in a reactor by double neutron capture of enriched ^{186}W (>90%) targets via the nuclear reactions, ^{186}W(n, γ)^{187}W(n,γ)^{188}W. High neutron flux (>8–10 × 10^{14}/cm^2/s) reactor is essential to produce high specific activities.

17.3.1.12 Holmium-166

^{166}Ho ($T_{½}$ 26.763 h) decays by β⁻ emission (E_{max} = 1.854 MeV)) to erbium-166, with useful γ emissions (81 KeV) for SPECT. Holmium is a transition metal and one of the elements in the lanthanide series and the chemistry is similar to that of lutetium. Several clinical applications for therapy are under investigation [23]. ^{166}Ho-DOTMP for multiple myeloma, and ^{166}Ho-EDTMP for bone pain palliation have been investigated.

^{166}Ho is most frequently produced via the ^{165}Ho(n, γ)^{166}Ho nuclear reaction (IAEA-TECDOC-1340). However, ^{166m}Ho ($T_{½}$ = 1200 years), a beta emitter may be produced as a radionuclidic impurity. The specific activity is NLT 75 mCi/mg. ^{166}Ho can also be produced by an indirect method via the ^{164,165}Dy(2n, γ)^{166}Dy → ^{166}Ho nuclear reaction. The cross-section of ^{164}Dy is extremely high (2650 b). The second neutron irradiation of the unstable ^{165}Dy is necessary to result in ^{166}Dy, which decays by beta emission to carrier-free ^{166}Ho. A ^{166}Dy → ^{166}Ho generator can provide on-site supply of high specific activity ^{166}Ho for targeted therapy.

17.3.1.13 Lead-212

^{212}Pb ($T_{½}$ = 10.6 h) is a β⁻ emitter but its interest in TAT as an in vivo generator comes from the fact that its first daughter, ^{212}Bi, is an α emitter with a short half-life of 60.6 min. Lead is classified as a post-transition metal with a weak metallic character and the preferred oxidation state is +2. ^{212}Pb is produced following the ^{228}Th decay sequence and can be obtained using ^{228}Th or ^{224}Ra-based generators.

17.3.2 Radionuclides-Emitting Alpha Particles

Alpha (α) particles are naked ^{4}He nuclei with 2 positive charges, consisting of 2 protons and 2 neutrons that are 7300 times heavier than electrons. Alpha particles are mostly emitted by heavy radioactive elements, such as radium, actinium, thorium, and uranium, and their daughters (Table 17.5). Alpha particles are ejected from the nucleus with much higher kinetic energy (5–9 MeV) compared to that of beta particles. In addition, alpha particles are monoenergetic as shown in Fig. 17.2b The range (<100 μm) of α particles in tissue is equivalent to only a few cell diameters. The short range of a particles is ideally suited for the treatment of small-volume cancer tissue. However, the energy distribution between the α particle and the recoiling daughter atom is typically 98 to 2%. The energy imparted to the daughter recoil atom can reach 100 keV [24], which is far higher than the binding energy of the strongest chemical bonds. As a result, the daughter nuclide may be released from the targeting vehicle chelator and diffuse into surrounding normal tissue and induce toxic effects.

Compared to beta emitters, α-particle emitters for TRT offers several important advantages. Alpha particles have higher kinetic energy (5–9 MeV) and higher LET in biological tissue. For example, ^{211}At has a mean LET of 97 KeV/μm, compared to the LET (0.22 keV/μm) of high-energy (2.2 MeV) beta particle of ^{90}Y. As a result, the probability of creating cytotoxic double-stranded breaks (DSBs) of DNA is much higher, and the relative biological effectiveness (RBE) is also significantly higher compared to that of beta

Table 17.5 The physical characteristics of alpha-emitting radionuclides for targeted therapy

Radionuclide	$T_{½}$	Daughter(s)		**α particle**		$β^-$ particle		γ-ray		X-ray	
	Days	Nuclide	$T_{½}$	MeV	%	MeV	%	MeV	%	KeV	%
^{227}Th	18.7	^{223}Ra	11.4 days	**6.0**	100			0.236	13	19	37
^{223}Ra	11.435	^{219}Rn		**5.7**	100			0.690	14	83	25
		^{219}Rn	3.96 s	**6.8**	79.4			0.271	10	16	1
		^{215}Po	1.78 ms	**7.4**	99.9						
		^{211}Pb	36.1 m			0.471	91	0.404	3.8		
		^{211}Bi	2.14 m	**6.6**	83.5	0.172	0.3	0.351	13		
		^{211}Po	0.516 s	**7.5**	98.9						
		^{207}Tl	4.77 m			0.492	99.7				
		^{207}Pb	Stable								
^{224}Ra	3.63	^{220}Rn		**5.7**	95.0			0.241	4.1		
		^{220}Rn	55.6 s	**6.3**	99.9						
		^{216}Po	0.15 s	**6.8**	99.9						
		^{212}Pb	10.6 h	–	–	0.0935	83	0.238	43.7	77	17.5
		^{212}Bi	60.6 m	**6.1**	25	0.834	55	0.727	6.7	15	7.0
		^{212}Po	0.3 μs	**8.8**	100						
		^{208}Tl	3.1 m			0.65	49	2.614	99.0		
		^{208}Pb	Stable								
^{225}Ac	10	^{221}Fr		**5.8**	50.7			0.1	1.0		
		^{221}Fr	4.8 m	**6.3**	83.3			0.218	11.4	17.5	2.0
		^{217}At	32.3 ms	**7.1**	99.9						
		^{213}Bi	45.6 m	**5.9**	1.9	0.492	66	0.440	26	79	1.8
		^{213}Po	3.72 μs	**8.4**	100						
		^{209}Tl	2.161 m			0.178	0.4	1.567	99.7	75	9.7
		^{209}Pb	3.253 h			0.198	100				
		^{209}Bi	Stable								
^{211}At	7.21 h	^{207}Bi		**5.9**	42					79	
		^{207}Bi	31.6 years			?		0.570			
		^{211}Po	0.52 s	**7.5**	98.9						
		^{207}Pb	Stable								
^{149}Tb	4.12 h	^{145}Eu		**4.0**	16.7	$β^+$, 0.64	83.3	0.352	29.4	43	26
		^{145}Eu	5.9 days			$β^+$, 0.74	1.7	0.894	66.0	40	40
		^{145}Sm	343.3 days					0.061	12.0	39	40
		^{145}Pr	17.7 years					0.072	2.0	37	71
		^{145}Nd	Stable								
		^{149}Gd	9.28 days					0.158	48.0	42	55
		^{149}Eu	93.1 days							40	40
		^{149}Sm	Stable								

Bold value indicates the alpha particle energy is very high

emitters. In addition, cytotoxicity of alpha particles is nearly independent of dose rate and oxygenation status of the cells. The oxygen enhancement ratio (OER), the ratio of dose required to kill a given fraction of cells in hypoxic vs. oxic conditions, decreases with increasing LET [25]. The OER reaches 1 with LET of 165 keV μm. Therefore, hypoxic and radioresistant tumors are more effectively killed by α radiation of LET >100 KeV/μm.

17.3.2.1 Astatine-211

^{211}At ($T_{½}$ 7.2 h) is an artificially produced α emitter which decays via a branched pathway to stable ^{207}Pb as shown in Fig. 17.3. ^{211}At decays directly (41.7%) to ^{207}Bi with the emission of an α particle (5.87 MeV), and ^{207}Bi decays by beta emission to ^{207}Pb. In the second branch ^{211}At first decays by EC (58.3%) to ^{211}Po which immediately decays by emission of an alpha particle (7.45 MeV) to ^{207}Pb. The EC decay of ^{211}At also leads to the generation

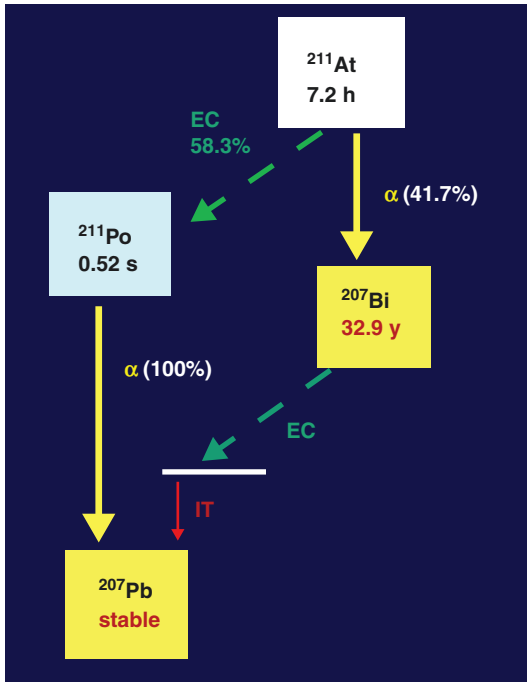

Fig. 17.3 At-211 decay results in the emission of 2 alpha particles with kinetic energies of 5.87 and 7.45 MeV

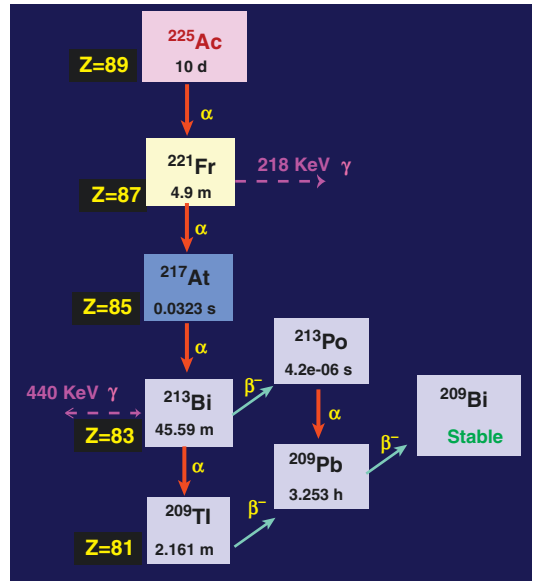

Fig. 17.4 Ac-225 decay results in the emission of 4 alpha particles (5.8–8.4 MeV) and 3 beta particles

of 77–92 KeV X-rays of polonium, which are suitable for SPECT imaging studies.

^{211}At is produced by cyclotron and α-particle bombardment via ^{209}Bi(α, 2n)^{211}At nuclear reaction using natural Bi-209 target. The thick target yield of ^{211}At is reported to be between 30 and 40 mCi/μA h at 28–29.5 MeV [21]. As the last member of the halogen family, astatine is the least electronegative in the halogen series and exhibits metallic properties. ^{211}At-labeled aromatic compounds are usually prepared by exchange halogenation or by electrophilic substitution on aromatic rings. ^{211}At has been extensively evaluated for alpha RT therapy in the last 3 decades [26].

17.3.2.2 Actinium-225

^{225}Ac is a pure α emitter with a half-life of 10 days, ^{225}Ac exhibits a complex decay scheme involving several radioactive isotopes (Fig. 17.4) before it reaches stable ^{209}Bi. ^{225}Ac and its daughters emit a total of four alpha particles. The two short-lived daughters, ^{221}Fr and ^{213}Bi emit useful γ photons (218 and 440 KeV). Quantitative measurement of ^{225}Ac activity in a dose calibrator is possible, when these two daughters are in secular equilibrium with the parent. From a radiobiology point of view, there is concern that the release of these two relatively long-lived daughters may result in excessive toxicity to normal organs. It is especially important to design the chelator system to form stable complexes with actinium and the daughters so that the α particle recoil energy does not break chemical bonds and let the daughters diffuse into surrounding normal tissues.

^{225}Ac is mainly produced by isolation and purification from ^{229}Th (T½ = 7340 years), which is a decay product of uranium-233 ($T_{½}$ = 165,000 years). ORNL is a major producer of ^{225}Ac based on Th-229 generator (Thorium cow). The potential of using low-energy cyclotrons (<20 MeV) based on ^{226}Ra(p, 2n)^{225}Ac nuclear reaction was first reported in 2005 [27]. A major challenge, however, with this cyclotron method is related to the preparation and handling of targets containing milligram amounts of ^{226}Ra ($T_{1/2}$ = 1600 years), and management of its gaseous decay product ^{222}Rn ($T_{1/2}$ = 3.8 days).

Large-scale production of ^{225}Ac has been investigated based on the spallation of ^{232}Th targets with highly energetic protons (>70 MeV).

The nuclear reaction ^{232}Th(p, x)^{225}Ac was studied at different proton energies and beam currents. In recent years, the routine production of ^{225}Ac has been successfully established within the United States, Department of Energy Tri-Lab (ORNL, BNL, LANL) effort. The main limitation of the process, however, is the coproduction of long-lived ^{227}Ac ($T_{1/2}$ = 21.8 years) at levels of 0.1–0.2% activity (at EOB) [28].

17.3.2.3 Bismuth-213

^{213}Bi ($T_{½}$ 45.6 m) is a hybrid α/β$^-$ emitter, and finally becomes stable ^{209}Bi. It decays by β$^-$ (97.9%) to ^{213}Po which immediately decays by α emission to ^{209}Pb. In the second branch, it decays by α emission (2.1%) to ^{209}Tl. In addition, the decay of ^{213}Bi is also accompanied by a 440 keV γ photon emission. ^{213}Bi is generally produced as a decay product of ^{225}Ac (Fig. 17.4). The ^{225}Ac → ^{213}Bi generator requires purified ^{225}Ac and uses an organic anion-exchange system (AG-MP 50 resin) capable of isolating ^{213}Bi from a HCl solution of ^{225}Ac. The most established strategy is based on the direct generator method, in which the parent ^{225}Ac in acidic solution (e.g., 0.05 M HNO_3) is strongly retained by the sorbent. Elution is performed generally with a mixture of 0.1 M HCl/0.1 M NaI to obtain ^{213}Bi in the form of $^{213}BiI_4^-$ and $^{213}BiI_5^{2-}$ that can be directly used for radiochemistry purposes [29] A commercial ^{225}Ac → ^{213}Bi generator is currently supplied by iTM, Germany.

17.3.2.4 Thorium-227

^{227}Th ($T_{½}$ 18.7 days) decays to stable ^{207}Pb with 6 intermediate radionuclide progenies and a total of 6 α particles (Fig. 17.5). Massive quantities of ^{227}Th can be obtained by the beta decay of ^{227}Ac ($T_{½}$ 21.8 years), the long-lived isotope of actinium, identified in the ^{235}U decay products. The routine production of ^{227}Th is based on ^{227}Ac → ^{227}Th generator. ^{227}Th emits an α particle with 5.9 MeV energy and 236 KeV γ photons, suitable for imaging studies. ^{227}Th and all its daughters would deposit up to 34 MeV of energy at the target site.

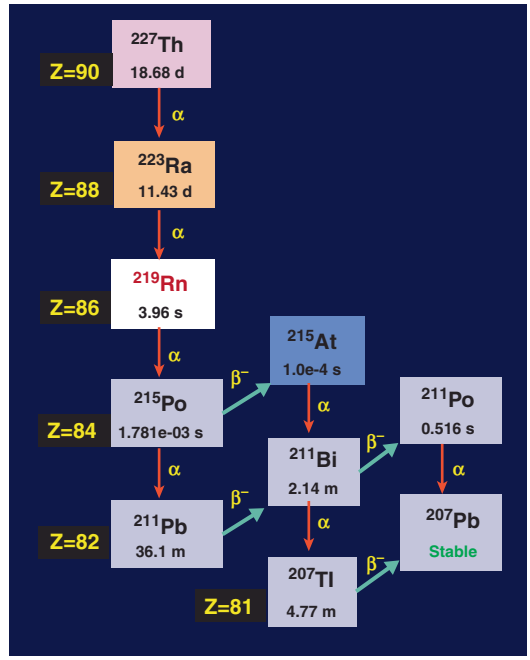

Fig. 17.5 Th-227 decay results in the emission of five alpha particles (5.7–7.5 MeV) and several beta particles. ^{223}Ra is the daughter nuclide obtained from ^{227}Th → ^{223}Ra generator

17.3.2.5 Radium-223

^{223}Ra ($T_{½}$ = 11.4 days) decays to stable ^{207}Pb with 5 intermediate radionuclide progenies and a total of 5 α particles (Fig. 17.5). ^{223}Ra is the first α emitter approved by the FDA in 2013 for the treatment of bone cancer in patients with prostate cancer. ^{223}Ra is a decay product of ^{227}Ac with a half-life of 21 years. Currently, the clinical and commercial production of $^{223}RaCl_2$ (Bayer Health Care Pharmaceuticals) involves ^{227}Ac and ^{227}Th isolation from a ^{231}Pa source (3.28×10^4 years) [26].

17.3.2.6 Radium-224

^{224}Ra ($T_{1/2}$ = 3.63 days) decays to ^{208}Pb with 6 intermediate radionuclide progenies (Fig. 17.6). In Europe, short-lived ^{224}Ra was used for more than 40 years in the early 1900s in treating tuberculosis and ankylosing spondylitis [30]. A major problem of the use of ^{224}Ra clinically, however, is due to the presence of 2 daughters ^{212}Pb ($T_{1/2}$ 10.64 h) and ^{212}Bi ($T_{1/2}$ 60.6 min) which will

migrate from the target site and diffuses into the surrounding normal tissue and deliver toxic radiation dose. ^{212}Pb decays by β⁻ emission to ^{212}Bi. Therefore, both these radionuclides, show potential for TAT, with ^{212}Pb being preferable to ^{212}Bi for clinical studies due to the longer half-life of ^{212}Pb, and because it can also generate ^{212}Bi in vivo, permitting more dose from ^{212}Bi progeny to be delivered to the target site.

17.3.2.7 Bismuth-212

^{212}Bi (T½ 60.6 min) is a hybrid α/β⁻ emitter and has two decay modes (Fig. 17.6). It decays by α emission (36%) to ^{208}Tl, which in turn decays by β⁻ emission to stable ^{208}Pb. In the second branch, it decays by beta emission (64%) to ^{212}Po, which immediately decays by alpha emission (100%) to stable ^{208}Pb. Both ^{212}Bi and ^{208}Tl also have extremely high-energy γ emissions not useful for imaging studies. ^{212}Bi is generally produced using either ^{224}Ra → ^{212}Bi generator or ^{212}Pb → ^{212}Bi generator. The parent ^{224}Ra first decays to ^{220}Rn gas, which is of great concern from a radiation safety perspective. The decay product ^{208}Tl emits 2.6 MeV photons, which increases radiation exposure to personnel. Because of these practical concerns, ^{213}Bi may not be ideal for clinical studies.

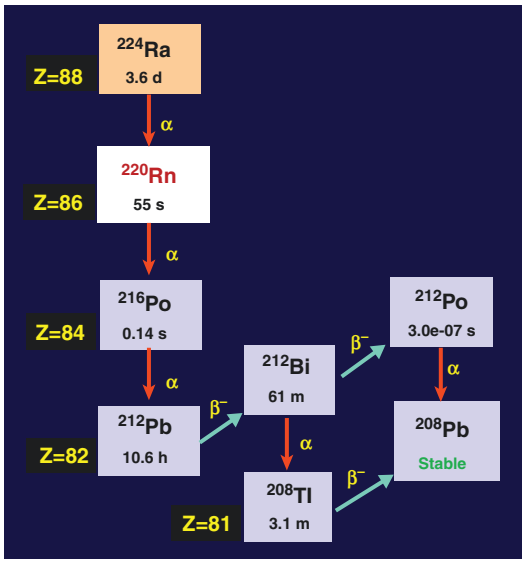

Fig. 17.6 Ra-224 decay scheme shows two radionuclides of interest. ^{212}Pb and ^{212}Bi. Both these two radionuclides are obtained using ^{224}Ra generator. While ^{212}Pb is not an alpha emitter, it is used as an in vivo generator for ^{212}Bi, which emits two alpha particles

17.3.2.8 Terbium-149

^{149}Tb ($T_{½}$ 4.1 h) decays by α emission as well as EC and positron emission. It ultimately decays to stable ^{145}Nd or ^{149}Sm. In the first branch, it decays to ^{145}Eu with the emission of α particles (4 MeV, 17.6%). In the second branch, ^{149}Tb decays to ^{149}Gd with the emission of positrons (E_{max} = 0.638 MeV, 83.3%). The decay scheme for ^{149}Tb is ideal to develop radiopharmaceuticals since it releases short-range α particles from only one radionuclide, with complementary positron emissions for PET imaging studies. Since there is only one α particle and no daughters with recoil energies, ^{149}Tb provides minimal toxicity [31]. ^{149}Tb can be produced in a cyclotron via ^{154}Gd(p, x)^{149}Tb spallation reaction using 70 MeV protons [32].

17.3.3 Radionuclides Emitting Low-Energy Electrons

Radionuclides that decay by electron capture (EC) or internal conversion (IC) emit electrons from the inner or outer shell electron orbits (Table 17.6). These electrons are called Auger electrons if they arise from higher shells and are called Coster-Kronig electrons if they originate from higher subshells. In contrast to β⁻ particles, the average kinetic energy of these electrons is very low. As a result, low-energy Auger electrons traverse short distances (<μm) in biological tissue and deposit the energy in the immediate site of the decaying radionuclide. Therefore, to realize the full therapeutic potential of Auger electron emitters in TRT, it is necessary for the radionuclides to target the nuclear DNA within the cell [33]. When low-energy electron emitters are localized in cellular DNA, their RBE is similar to that observed with α-particle emitters [34].

Table 17.6 Radionuclides emitting low-energy Auger and internal conversion electrons

	$T_{½}$	Auger electrons			Internal conversion (IC) electrons		
Radionuclide	Days	AEs/ Decay	E_{avg}/AE KeV	E_{avg}/decay KeV	IC-Es / Decay	E_{avg}/IC-E KeV	E_{avg}/decay KeV
^{67}Ga	3.25	5	1.3	6.6	0.3	14.1	29.1
^{111}In	2.79	7.4	0.9	6.9	0.2	176.1	27.9
^{201}Tl	3.04	20.9	0.7	14.8	0.9	32.9	29.9
^{123}I	0.542	13.7	0.5	7.2	0.2	222.6	21
^{125}I	60.0	23	0.5	12.0	0.9	7.7	21
^{195m}Pt	4.0	36.6	0.6	23.1	2.8	58.1	161.5

Table modified from [33]

17.3.4 In Vivo Radionuclide Generators

Most of the radionuclides used in the development of diagnostic or therapeutic radiopharmaceuticals decay to a stable isotope of the same element or an isotope of another element. For example, the diagnostic nuclide F-18 decays by positron emission to stable oxygen-18. The therapy nuclide, I-131 decays by beta emission to stable Xe-131 inert gas. A radionuclide (parent) which decays to another radionuclide (daughter) or a series of radionuclides (decay chain) can be classified as in vivo radionuclide generators. ^{223}Ra dichloride (xofigo®) is a classic example of an in vivo generator since it generates four short-lived α-emitting daughters (^{219}Rn, ^{215}Po, ^{211}Bi, and ^{211}Po) at the target site following intravenous administration.

The term in vivo generator was first used to describe the use of targeted mAbs labeled with long-lived parent radionuclides that decay into short-lived daughter radionuclides. The concept is to combine the long half-life of the parent with the high decay energy of the daughter to achieve high-dose targeted radiotherapy [35–37]. Overall, the advantage of in vivo generators is to combine nuclear and chemical properties of the parent and daughter nuclides to better diagnose or treat physiological conditions. Some of the therapeutic radionuclide in vivo generator systems are listed in Table 17.7.

The most important consideration when employing an in vivo generator is the instability of the radiopharmaceutical that can result from the chemical transformation of one element to another. There are two opportunities for the daughter to separate from the parent, either because of the elemental differences between the parent and daughter or because of the physical and chemical disruption caused by the nuclear decay itself [35]. The recoil of the daughter nucleus could provide sufficient energy to dislodge the daughter from strong polydentate chelates. If the half-life of the daughter(s) is longer, they could diffuse into the surrounding normal tissue and deliver toxic radiation doses. For example, ^{227}Th, ^{223}Ra, and ^{225}Ac generate several daughters with half-lives long enough to diffuse into blood circulation and the normal tissues [38].

17.3.5 Mechanism and Biological Effects

The mechanism of action for radionuclide therapy is radiation-induced killing of cells. The ionizing radiation (especially the highly energetic particles such as electrons, protons, neutrons, and α particles) forms ions, the electrically charged particles, and deposits energy in the cells of the tissues it passes through. The energy dissipated per ionizing event is about 33 eV, which is more than enough to break a strong chemical bond, such as a C–C bond (4.9 eV). This deposited energy can kill cancer cells or cause genetic changes resulting in cancer cell death. Although radiation damages both normal cells as well as cancer cells, normal cells usually can repair themselves at a faster rate and retain its normal function status than the cancer cells. In addition,

Table 17.7 Radionuclide in vivo generator systems useful for targeted therapy

Parent				Daughter(s)				
Nuclide	$T_{½}$	Decay	E (MeV)	Nuclide	$T_{½}$	Decay	E (MeV)	Recoil E (KeV)
^{166}Dy	3.4 days	β⁻	E_{max} 0.481	^{166}Ho	1.12 days	β⁻	E_{max} 1.85	
^{212}Pb	10.64 h	β⁻	E_{max} 0.574	^{212}Bi	1.01 h	α	6.1	
						β⁻	E_{max} 2.254	
				^{212}Po	0.3 μs	α	8.8	
				^{208}Tl	3.1 min	β⁻	E_{max} 1.803	
^{211}At	7.21 h	α	5.9	^{211}Po	0.52 s	α	7.5	
^{227}Th	18.67 days	α		^{223}Ra	11.435 days	α	5.7	108.4
^{223}Ra	11.435 days	α	5.7	^{219}Rn	3.96 s	α	6.8	104.5
				^{215}Po	1.78 ms	α	7.4	126.9
				^{211}Pb	36.1 min	β⁻	E_{max} 1.361	
				^{211}Bi	2.14 min	α	6.6	140.1
				^{211}Po	0.516 s	α	7.5	
				^{207}Tl	4.77 min	β⁻	E_{max} 1.423	
^{225}Ac	10.0 days	α	5.8	^{221}Fr	4.8 min	α	6.3	105.5
				^{217}At	32.3 ms	α	7.1	116.9
				^{213}Bi	45.6 min	α	5.90	132.8
						β⁻	E_{max} 1.427	
				^{213}Po	3.72 μs	α	8.4	160.4
				^{209}Tl	2.161 min	β⁻	E_{max} 3.97	
				^{209}Pb	3.253 h	β⁻	E_{max} 0.644	

cancer cells in general are not as efficient as normal cells in repairing the damage caused by radiation treatment resulting in differential cancer cell killing [39].

17.3.5.1 Linear Energy Transfer (LET)

Radiation-induced ionization in the cells is the major cause of the biological effects of radiation. Specific ionization (SI) means the total number of ion pairs produced per unit length of the path of the incident radiation. For heavily charged particles, the SI increases with decreasing energy of the charged particles because of the increased probability of interaction at low energies. The quantity of linear energy transfer (LET) is the amount of energy deposited by the radiation per unit length of the path (KeV/μm). Low LET radiation (X-rays, γ-rays, electrons) deposits relatively a small quantity of energy while high LET radiation (protons, neutrons, and α particles) deposits higher energy in the targeted areas (Table 17.8).

The Bragg curve (Fig. 17.7) is a plot of the energy loss (or LET) of a charged particle during its travel through the matter. For protons and, α-rays, the peak (called Bragg peak) occurs immediately before the particles come to rest. In biological tissue, the complete energy of an α particle is dissipated in <100 μm (i.e., only a few cell diameters). The alpha particle LET, however, is inversely related to the energy and most of the alpha particle energy loss occurs at the end of the

Table 17.8 Linear energy transfer (LET) and relative biological effectiveness (RBE) of radionuclide emissions

Radiation type	LET (KeV/μm)	RBE	Energy W_R
^{60}Co, γ-rays	0.2	0.8–0.9	1.0
LINAC X-rays (6–15 MeV)	0.3	~0.8	1.0
β particles (1 MeV)	0.3	0.9	1.0
X-rays, 250 kVp (standard)	2.0	1.0	1.0
Protons (150 MeV)	0.5	1.1	2.0
Neutrons	0.5–200	1–2	2.5–5.0
α-particles	50–200	5–10	20.0

Table modified from [40, 41]

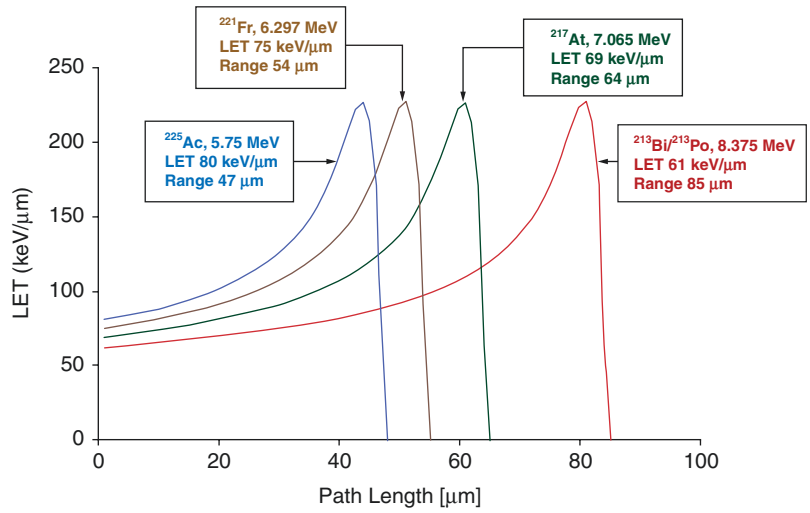

Fig. 17.7 The Bragg curves for the four alpha particles emitted from the decay of ^{225}Ac and the daughter radionuclides. The higher the kinetic energy of the alpha particle, the lower the LET but, the longer the range of the particle in the tissue. (Figure modified from [42])

path, and at that moment the LET of the alpha particle increases to 200–250 keV/µm. The higher energy alpha particles lose less energy, or they have lower LET and vice versa.

17.3.5.2 Absorbed Dose vs. Equivalent Dose

The energy deposited by radiation in a target is called the "absorbed dose (D_T)", which is expressed as the total energy deposited in a unit volume of mass (m). The SI unit for D_T is the "***Gray***", which is equal to 1 J of energy absorbed in 1 kg of mass (any type of matter, living or non-living). When the mass of matter is biological tissue, the absorbed dose is given by another name, the "equivalent dose (H_T)", which is defined as the product of DT (Grays) and a radiation weighing factor, (W_R) for a specific radiation type. (W_R, formerly known as quality factor, Q). The SI unit for equivalent dose is the "***Sievert***", which has the same units as the Gray.

$$\text{Equivalent dose}\left(H_T\right) = \text{Absorbed dose}\left(D_T\right) \times \text{Radiation weighing factor}\left(W_R\right) \tag{17.3}$$

17.3.5.3 Relative Biological Effectiveness (RBE)

$$RBE = D_X / D_R \tag{17.4}$$

The absorbed dose (Gy) and equivalent dose (Sv) can be poor indicators of the biological effect of radiation, such as cell killing, since the biological effect can depend on the type of radiation, energy, and type of tissue. In radiobiology, RBE is an empirical value that varies depending on the type of ionizing radiation, the energies involved, the biological effects, and the oxygen effect. The RBE can help give a better measure of the biological effect of radiation. RBE is the ratio of biological effectiveness of one type of ionizing radiation relative to another, given the same amount of energy. The RBE for radiation of type *R* on a given tissue is defined as the ratio where D_X is a reference absorbed dose of radiation of a standard type X, and D_R is the absorbed dose of radiation of type R that causes the same amount of biological damage. Distinct types of radiation have different biological effectiveness mainly because they transfer their energy to the tissue in different ways. As LET increases, relative biological effectiveness (RBE) increases and maximizes around 100 KeV/µm, and then RBE decreases with LET. Radiation weighing factors (W_R) used to convert absorbed dose to equivalent dose are not dependent on the type of tissue and, therefore, should not be used to estimate the RBE. As shown in Table 17.3 above, WR may be higher for particles.

17.3.6 Biological Effectiveness of Radionuclide Therapy

Radiation damage to the cell can be caused by the direct or indirect action of biological molecules [43]. In the direct action, the radiation hits the DNA molecule directly, causing single-stranded breaks (SSB) or double stranded breaks (DSB), disrupting the molecular structure (Fig. 17.8). Such structural change leads to cell damage or even cell death. This process becomes predominant with high-LET radiations, such as α-particles and neutrons, and high radiation doses. In the indirect action, the radiation hits the water molecules generating reactive oxygen species (ROS), such as hydrogen peroxide (H_2O_2) and free radicals (characterized by an unpaired electron), such as hydroxyl ($HO^{\bullet}$) group. In addition, indirect effects of radiation may also involve reactive nitrogen species (RNS). All the reactive molecules are toxic and can have many effects, including the oxidation of biological macromolecules and activation of intracellular signaling pathways. It has been found that the majority of radiation-induced damage results from the indirect action mechanism because water constitutes nearly 70% of the composition of the cell [44]. A widely accepted dogma in the field of radiation biology is that effects of ionizing radiation, such as cell death, chromosomal aberrations, DNA damage (both SSB and DSB), mutagenesis, and carcinogenesis, result from direct or indirect ionization of cell structures, particularly DNA. Overall, radiation-induced DNA damage is believed to activate a variety of signaling pathways leading to cell death, as well as accelerated senescence.

Recent investigations have challenged the classical DNA-centric view of radiation injury by demonstrating that proteins are also critical radiation targets that influence cell death mechanisms. In some cases, radiation-induced death by protein damage is proposed to be a consequence of reduced DNA repair fidelity, indirectly decreasing cell viability. In addition, recent studies also suggest that the detrimental effects of ionizing radiation are not restricted only to the irradiated cells but, also, to non-irradiated bystander or even distant cells manifesting various biological effects [45]

The molecular mechanisms of radiation-induced cellular injury, or biological effectiveness (cell killing) of radiation, however, depends on the LET of radiation, total dose, dose rate, and radio-sensitivity of the targeted cells or tissues. Low LET radiation (X-rays, γ-rays, electrons) deposits a relatively small quantity of energy while high LET radiation (protons, neutrons, and α particles) deposits higher energy in the targeted areas (Table 17.8). Radiation is generally more damaging in rapidly dividing cells and in undifferentiated cells. For example, untransformed epithelial cells of the gastrointestinal tract and progenitor cells of the hematopoietic system, which have rapid turnover rates, are generally more radiosensitive than the non-dividing neurons of the central nervous system. This differential proliferative capacity corresponds to the induction of Hematopoietic Syndrome at lower radiation exposures (0.7–10 Gy) compared to doses required for inducing Central Nervous System Syndrome (>50 Gy) [46].

17.3.6.1 Mechanisms of Cell Death

Radiation exposure to cells has been demonstrated to result in a variety of mechanisms of cell death, including necrosis, apoptosis, or autophagy. The basis for cellular selection for each mode, however, depends on a range of factors, including the specific cell type involved, the dose of radiation absorbed by the cell, and whether it is proliferating and/or transformed [46]. Many cancer cells, including lung, prostate, immortalized keratinocytes, and colon cancer cells, commit to apoptotic cell death when exposed to radiation ranging from 1 to 20 Gy. Low doses of radiation (0.1–2 Gy) have been demonstrated to induce apoptosis in human skin organotypic culture and murine epidermal cells.

The main goal of radiation therapy is to deprive cancer cells of their multiplication potential and eventually kill the cancer cells. Cancer cells whose DNA is damaged beyond repair stop dividing and die. Radiation therapy does not kill cancer cells right away. It takes hours, days, or weeks of treatment before cancer cells start to die after which cancer cells continue dying for weeks to months after radiation therapy ends. A deeper

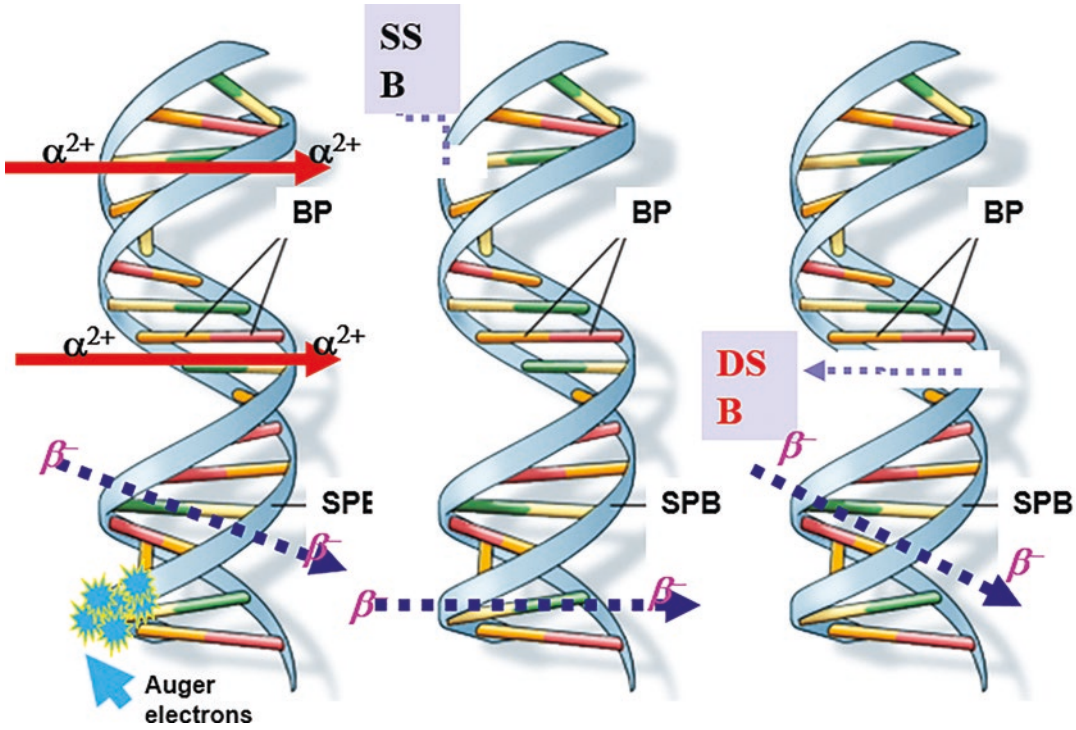

Fig. 17.8 Illustration of the interaction of radiation (β^-, α particles, and *Auger* electrons) with DNA. Alpha particles induce both single-strand and double-strand breaks in DNA but, beta particles pass through the double helix. Auger electrons will deposit all their energy very close to their origin

knowledge of the underpinning mechanisms and their interplay will reveal opportunities for enhancing the overall anti-tumor activity of RNT.

17.4 Design of Radiopharmaceuticals for TRT

17.4.1 Ideal Characteristics

TRT involves the use of a radiolabeled molecule to selectively deliver a cytotoxic level of radiation to a disease site. Advances in radionuclide production of alpha and beta emitters, tumor biology, recombinant antibody technology, and radiochemistry have led to a flurry of activity in the development and clinical application of target-specific therapeutic radiopharmaceuticals. In summary, an ideal radiopharmaceutical for

TRT, under ideal conditions, must have the following characteristics:

- High specificity and affinity for tumor cells
- In vivo stability in blood and within the tumor tissue with minimal metabolite formation
- Rapid blood clearance (to minimize bone marrow dose)
- Rapid targeting and significant retention of the therapeutic radionuclide (3–4 half-lives of the radionuclide) within the tumor
- Homogeneous radiation dose deposition within the tumor
- Rapid excretion from the body with minimal uptake and retention by normal tissues and cells
- Minimal hematologic toxicity in order to increase the maximum tolerated dose (MTD)
- to preserve dose-rate effect
- Acceptable toxicity to liver, spleen, and kidney
- No radiation-induced biologic effects such as mutation or transformations leading to secondary cancers.

To meet all the requirements described above, the design and development of a successful therapeutic radiopharmaceutical for TRT (Fig. 17.1) require the following steps:

1. Based on preclinical work, identifying the most appropriate and specific biological target (receptor or an antigen on the cancer cell membrane) for the therapy of a specific cancer.
2. Selection of a targeting vehicle (peptide, small organic molecule, monoclonal antibody, or a particle such as liposome or a nanoparticle) with high affinity and specificity for biological target.
3. Identifying an appropriate therapeutic radionuclide for a specific cancer tissue and appropriate to radiolabel the ideal targeting vehicle.
4. Careful design of the binding moiety (targeting vehicle-spacer-linker-chelate) with optimal biodistribution and pharmacokinetic parameters.
5. All the above steps require careful multistep matching of the (a) target and the ligand molecule, (b) the ligand and the radionuclide, (c) the tumor and radionuclide, and, finally, (d) the radionuclide and the chelator.

17.4.2 Selection of Therapeutic Radionuclide

Various radionuclides used for therapy are listed in Table 17.3. Although numerous radionuclides have potential applications in radionuclide therapy, only a very few radionuclides possess favorable physical, chemical, and biological characteristics which would identify them as practical for clinical use. Physical characteristics include physical half-life, type of emissions, energy of the emissions, daughter products, method of production, and radionuclidic purity. Biochemical characteristics include tissue targeting, retention of radioactivity in the tumor, in vivo stability, and toxicity.

The ideal radionuclides for therapy are those with an abundance of non-penetrating radiations, such as charged particles (α^{2+}, β^-, *and Auger electrons*), and lack of penetrating radiations (γ or X-rays). While penetrating radiation is not essential for TRT, a small amount or abundance with an appropriate energy (100–400 KeV) may be useful for imaging studies to demonstrate tumor localization or altered biodistribution.

The energy of the charged particle determines the amount of energy deposited in each volume of the tissue. Therefore, the choice of a particular radionuclide is strongly dependent on the LET value and tissue range of emissions. Each type of particle emitted by the radionuclide has a different range and effective distance. The higher the LET of a specific radionuclide, the greater the relative biological effectiveness (RBE). The β^- particles, Auger electrons, and conversion electrons have the same mass but, different kinetic energy and different ranges (0.1–3.0 mm) in tissue. All electrons have low LET values (0.2 keV/μm) and their RBE is unity. In contrast, α particles are 8000 times heavier and have very high LET values (40–100 KeV/μm), and therefore the RBE values can be 5–10 depending on the tissue. When a therapy radiopharmaceutical has a nonuniform distribution within the tumor (>1 mm), radionuclides with high-energy β^- particles deposit energy in cells that do not take up the radioisotope, by the crossfire effect. Therefore, for large-volume tumor tissue, radionuclides with β^- emission are appropriate. In contrast, for the treatment of microscopic disease (<1.0 mm in diameter), α particles are ideal since they deposit their energy (5–9 Mev) over short distances. Radionuclides with Auger electrons or other low-energy electrons have a short range and, if the radionuclide is localized in the nucleus, most of the energy will be deposited locally and potentially damage cellular DNA.

The physical half-life ($T_{½p}$) of the therapeutic radionuclide is important since the time course of irradiation of a target is related to both the physical half-life and biological turnover or biological half-life ($T_{½b}$) of the radiopharmaceutical. One must select an appropriate radionuclide depending on the carrier molecule used to develop the therapeutic agent. For example, with an intact antibody molecule, radioisotopes with medium

half-life (3–10 days) are preferable, while with small molecules and peptides, the half-life of the radionuclide may not be a major factor to consider.

17.4.3 Theranostic Pair of Radionuclides

The concept of "theranostics" describes a clinical management system that allows the combined diagnosis, treatment, and follow-up of a disease in order to identify a sub-population of patients most likely to benefit from a targeted therapy in accordance with their "molecular profile". In personalized medicine, diagnostic molecular imaging (using SPECT or PET) is often employed for selecting appropriate and optimal therapies based on the context of a patient's genetic content or other molecular or cellular analysis to look at a patient on an individual basis that will allow for a more accurate diagnosis and specific treatment plan. In nuclear medicine, theranostics is a personalized approach to treating cancer, using the same or similar molecules for both imaging (diagnosis) and targeted therapy. After selecting a specific targeting vehicle, a diagnostic agent is prepared by attaching a radionuclide for PET or SPECT imaging study. The same targeting vehicle is also labeled with an appropriate therapeutic radionuclide-emitting beta, alpha or Auger electrons. It is important that the biodistribution, pharmacokinetics, and tumor uptake of both diagnostic and therapeutic agents are similar. The concept of theranostics was first introduced in the 1990s, however, ^{123}I or ^{131}I sodium iodide for diagnostic studies followed by treatment of thyroid disease with ^{131}I sodium iodide has been in clinical use for more than 70 years. Also, several laboratories developed ^{111}In-labeled octreotide as a chemical and biological surrogate of a therapeutic agent ^{90}Y-labeled octreotide since both radionuclides are trivalent metals.

Since ^{111}In imaging studies (planar and SPECT) did not provide quantitative data on radiation dosimetry in individual patients, researchers in Julich Germany came up with the idea of combining PET and radionuclide therapy by using a pair of radionuclides of the same element, one emitting positrons, and the other β^- particles (Table 17.9). ^{86}Y, a positron emitter was developed to perform patient specific dosimetry in patients receiving ^{90}Y-labeled therapeutic agent [47, 48].

17.4.4 Biological Target and Targeting Vehicle

Several biological targets expressing tumor-specific antigens or cell surface receptors are summarized in Tables 17.10 and 17.11. The targeting vehicles are small organic molecules (such as amino acids, MIBG, and steroid hormones), bioactive peptides, proteins or antibodies, and antibody fragments as shown in Tables 17.1 and 17.2. In the design of a target (binding site) specific radiopharmaceutical (Fig. 17.1), the choice of a biological target in the tumor tissue, however, depends on the following key factors:

- The accessibility of the target for the ligand is an important consideration. In this context, the microscopic environment of the target, including tumor vascularity, permeability, and oxygenation would all contribute to the net uptake of the radiopharmaceutical by the tumor.
- The number of binding sites (B_{max}) per tumor cell and the relative distribution and the expression of target molecules within the tumor tissue during each phase of the cell cycle. The concentrations of tumor-associated antigens and receptors among tumors from patients with a particular type of malignancy can vary from over 10^5 molecules per cell to undetectable levels. In addition, wide variations in antigen or receptor expression have been reported both, within the cells of a particular tumor, as well as between different tumors from the same patient.
- The expression of binding sites in the nontarget sites, such as blood and soft tissues (liver, kidney, spleen, and muscle).

Table 17.9 Theranostic radionuclides for imaging and therapy

Radionuclide for therapy						Radionuclide for PET					
Nuclide	*T½*	Decay	E_{max}	γ-rays	%	Nuclide	*T½*	Decay	E_{max}	γ-rays	%
			MeV	KeV					MeV	KeV	
^{131}I	8.02 days	*β⁻ (100)*	0.607	364.5	82	^{124}I	4.18 days	β⁺ (22)	2.14	603	61
										723	10
^{90}Y	2.70	β⁻ (100)	2.29	–	–	^{86}Y	14.7 h	β⁺ (33)	2.34	627.8	32.6
										1077	82.5
										1153	30.5
^{67}Cu	2.58 days	β⁻ (100)	0.577	184.6	48.6	^{64}Cu	12.7 h	β⁺ (17.8)	0.653		
								β⁻ (38.4)	0.571	1346	0.53
								EC(43.8)			
^{47}Sc	3.35 days	β⁻ (100)	0.610	159	68	^{44}Sc	3.9 h	β⁺ (94.3)	1.470	1157	99.9
^{89}Sr	55.5 days	β⁻ (100)	1.470	–	–	^{83}Sr	32.4 h	β⁺ (94.3)	1.274	381.3	19.6
^{161}Tb	6.9 days	β⁻ (100)	0.590	74.6	9.8	^{152}Tb	17.5 h	β⁺ (18.0)	2.500	344.3	57
^{149}Tb	4.1 h	α (16.7)	α 5.83	165	27.8	^{149}Tb	4.1 h	β⁺ (4.3)	0.600	165	28
		EC (79)		352	33			EC (79)		352	33
^{177}Lu	6.73 days	β⁻ (100)	0.498	113	6.4	^{68}Ga	67.6 min	β⁺ (90)	2.921	1077	3.0
				208	11	^{111}In	2.805 days	EC (100)	–	171.3	90
										245.4	94

Table 17.10 Tumor-specific biological targets (antigens and proteins) to develop therapeutic radiopharmaceuticals

Target	Patient population
CD20	Non-Hodgkin's lymphoma
Prostate-specific membrane antigen (PSMA)	Prostate cancer
Epidermal growth factor, EGFR (HER1)	Colorectal cancer
Human epidermal growth factor-1 (HER2)	Breast cancer
Human epidermal growth factor-3 (HER3)	Solid tumors
Carcinoembryonic antigen (CEA)	Colorectal cancer
CD-22	Non-Hodgkin lymphoma
CD-45	Acute myelogenous leukemia (AML)
CD-33	Acute myelogenous leukemia (AML)
Mesothelin (MSLN)	Ovarian or prostate cancer
Prostate stem cell antigen (PSCA)	Bladder, pancreatic, or prostate cancer
Placental growth factor (PLGF)	Glioblastoma multiforme
PD-1	Non-small-cell lung cancer (NSCLC), melanoma
PD-L1	Bladder cancer, NSCLC, triple-negative breast cancer (TNBC)
Transforming growth factor β (TGFβ)	Glioma
Vascular endothelial growth factor-A (VEGF-A)	Breast cancer, glioma, MM, NET, NSCLC, RCC

CD cell-surface differentiation antigen

Table 17.11 Peptide receptors as biological targets to develop therapeutic radiopharmaceuticals

Peptide	Receptor/ subtype	Tumor expression
Somatostatin	SSTR I–V	Neuroendocrine tumor, small cell lung, prostate cancer, breast cancer, colorectal carcinoma, gastric cancer, hepatocellular carcinoma
Bombesin	GRP-bombesin	Prostate, breast, small cell lung cancer (SCLC), gastric, ovarian, colon, and pancreatic cancers
	EGFR	Lung, breast, bladder, and ovarian cancers
Substance P	NK1	Glial tumors, astrocytomas, medullary thyroid cancer (MTC), and breast cancer
VIP	VPAC1	GI and other epithelial tumors
Integrins	$\alpha_V\beta_3$ integrin	Insulinomas, activated endothelial cells, glioblastomas, ovarian cancer.
CCK/gastrin	CCK2	MTC, insulinoma, SCLC, GISTs
Glucagon-like peptide 1 (GLP-1)	GLP-1-R	Insulinoma, gastrinoma
Neuropeptide-Y	NPY-R	Breast, ovarian, and adrenal tumors
Neurotensin	NT-R1	Exocrine pancreatic cancer, meningioma, Ewing sarcoma, and prostate cancer breast, colon, pancreatic, lung cancer

17.4.5 Radiolabeling Methods

Among the radionuclides listed in Table 17.3, ^{131}I, and ^{211}At belong to the halogen family (Group 17 in the periodic table). ^{211}At, however, is also regarded as a metalloid since it shares certain chemical properties with metals. All other radioisotopes listed are metals. The radionuclide production and the chemistry of halogens and radiometals are discussed in greater detail in Chaps. 8 and 18 of this book and in several review articles [49–52].

The labeling of peptides with radionuclides can be performed by direct labeling, with the addition of a prosthetic groups. Direct labeling is the method used to label peptides without using intermediates, such as BFCs. Direct labeling techniques are gen-

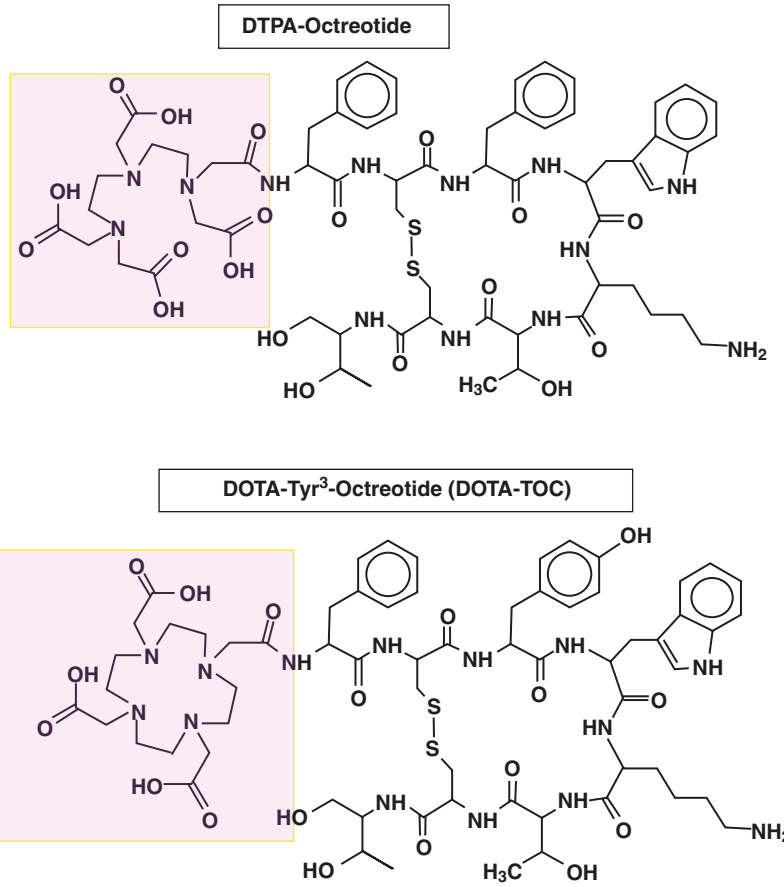

Fig. 17.9 Chemical structure of DTPA-Octreotide and DOTA-Tyr^3-octreotide (Dotatoc)

erally used mostly for radioiodination and in some cases labeling with Tc-99m. Prosthetic groups are small molecules which are able to bind with radionuclides in one site of the structure, and simultaneously with a peptide at a second site. Prosthetic groups are bifunctional agents that consist of a suitable site for radioiodination or fluorination and functional groups to allow covalent attachment of the peptide. Radiometals specifically require bifunctional chelating agents (BFC or BFCA) to obtain the best conjugation of radiometal with peptides. The bifunctional nature of the chelators means that they can coordinate (form a complex) a metal ion and can also be attached to the peptide. The most common chelating agents used for the development of radiolabeled small molecules, peptides, and proteins are analogs of DTPA and DOTA. The chemical structures of somatostatin analogs (octreotide and Tyr3-octreotide) conjugated with acyclic and macrocyclic BFCs are shown in Fig. 17.9. The design and development of radiolabeled peptides is discussed in greater detail in Chap. 20.

17.5 Therapy Radiopharmaceuticals Approved for Clinical Use

The therapy radiopharmaceutical may be a simple inorganic ion, metal complex, or particles. For TRT to be truly effective and specific, the carrier molecule or the targeting vehicle (ligand or vector), ideally, seeks the tumor cells and delivers the radionuclide to the tumor cells by specific binding to a target site, either on the cell surface or within the tumor cell. The selection of the targeting vehicle (such as antibodies and peptides)

and the preparation of target-specific therapeutic radiopharmaceutical (Fig. 17.1) involve complex design strategies.

17.5.1 Inorganic Ions

A classic example of TRT is the use of ^{131}I as sodium iodide (I^-) for the post-surgery treatment of thyroid cancer. The negatively charged radioiodide[^{131}I]I^- ion selectively accumulates in thyroid cancer cells by active transport via an ion pump known as sodium iodide symporter (SIS). In this mechanism, the radionuclide as iodide ion is the active ingredient of the radiopharmaceutical and no specific ligand or carrier is required.

Similarly, with the calcium analogs, ^{89}Sr chloride and ^{223}Ra chloride, the positively charged (cationic) $^{89}Sr^{2+}$ ion and $^{223}Ra^{2+}$ ion follow the biochemical pathway of calcium within the bone and localize in the hydroxyapatite ($Ca_{10}(PO_4)_6(OH)_2$), the mineral content of bone. These ions are preferentially taken up into bone metastases with increased bone turnover and no specific carrier is required to bind to the osteoblastic bone formation at the metastatic sites.

17.5.1.1 Sodium Iodide I 131 Solution

Sodium Iodide I 131 (Na I-131) Solution Therapeutic [53] is supplied for oral administration as a stabilized aqueous solution. The solution is available in vials that contain from 185 to 5550 MBq (5–150 mCi) iodine-131 at the time of calibration. Sodium Iodide I 131 Solution Therapeutic is packaged in shielded screwcap 15 mL vials. The solution contains 0.1% sodium bisulfite and 0.2% edetate disodium as stabilizers, 0.5% sodium phosphate anhydrous as a buffer, and sodium iodide I-131 at concentrations of 185 or 925 MBq (5 or 25 mCi) per milliliter. The pH has been adjusted to between 7.5 and 9. The iodine-131 utilized in the preparation of the solution contains not less than 99% iodine-131 at the time of calibration.

Indications and Usage: Sodium Iodide I 131 Solution is indicated for the treatment of hyperthyroidism and thyroid carcinomas that can accumulate radioiodide. Palliative effects may be observed in patients with advanced thyroid malignancy if the metastatic lesions take up iodide.

Mechanism of Action: Taken orally, sodium iodide I-131 is rapidly absorbed and distributed within the extracellular fluid of the body. The iodide is concentrated in the thyroid via the sodium/iodide symporter and, subsequently, oxidized to iodine. The destruction of thyroidal tissue is achieved by the beta emission of sodium iodide I-131.

Pharmacodynamics: The therapeutic effects of sodium iodide I-131 are a result of the ionizing radiation absorbed by the thyroidal tissue. Tissue damage is the result of a direct insult to molecules by ionization and excitation and the consequent dissociation of those molecules. About 90% of local irradiation from sodium iodide I-131 is the result of beta radiation and 10% is the result of gamma radiation.

Pharmacokinetics: After oral administration, sodium iodide I-131 is absorbed rapidly from the upper gastrointestinal tract (90% in 60 min). The pharmacokinetics follow that of unlabeled iodide. After entering the bloodstream, the iodide is distributed into the extra-thyroidal compartment. From here it is predominantly taken up by the thyroid or excreted renally. In the thyroid, the trapped iodide is oxidized to iodine and organified. The sodium/iodide symporter (NIS) is responsible for the concentration of iodide in the thyroid. This active transport process is capable of concentrating iodide 20–40 times the plasma concentration under normal circumstances, and this may increase tenfold in the hyperthyroid state. NIS also mediates active iodide transport in other tissues, including salivary glands, nasolacrimal duct, lacrimal sac, gastric mucosa, lactating mammary gland, and the choroid plexus. The non-thyroidal iodide transporting tissues do not have the ability to organify accumulated iodide.

Drug Interactions: Many pharmacologic agents interact with sodium iodide I-131. These agents (anti-thyroid drugs, thyroid hormones, iodine-containing medications, X-ray contrast agents, topical iodide, and several drugs) may affect the iodide protein binding and alter the iodide pharmacokinetics and pharmacodynamics.

17.5.1.2 Metastron™ (Strontium-89 Chloride Injection)

Metastron is a sterile, non-pyrogenic, aqueous solution of Strontium-89 Chloride for intravenous administration. The solution contains no preservatives. Each milliliter contains 10.9–22.6 mg of strontium Chloride. The radioactive concentration is 37 MBq/mL (1 mCi/mL), and the specific activity is 2.96–6.17 MBq/mg (80–167 μCi/mg) at calibration. The pH of the solution is 4–7.5 [54].

Indications and Usage: Metastron (Strontium-89 Chloride Injection) is indicated for the relief of bone pain in patients with painful skeletal metastases.

Dosage and Administration: The recommended dose of Metastron is 148 MBq (4 mCi), administered by slow intravenous injection (1–2 min). Alternatively, a dose of 1.5–2.2 MBq/kg (40–60 μCi/kg) body weight may be used. Repeated administrations of Metastron should be based on an individual patient's response to therapy, current symptoms, and hematologic status, and are generally not recommended at intervals of less than 90 days.

Mechanism of action: Following intravenous injection, soluble strontium compounds behave like their calcium analogs, clearing rapidly from the blood and selectively localizing in bone mineral. Uptake of strontium by bone occurs preferentially in sites of active osteogenesis; thus, primary bone tumors and areas of metastatic involvement (blastic lesions) can accumulate significantly greater concentrations of strontium than surrounding normal bone.

Pharmacokinetics: Strontium-89 Chloride is retained in metastatic bone lesions much longer than in normal bone, where turnover is about 14 days. In patients with extensive skeletal metastases, well over half of the injected dose is retained in the bones. Excretion pathways are two-thirds urinary and one-third fecal in patients with bone metastases. Urinary excretion is higher in people without bone lesions. Urinary excretion is greatest in the first 2 days following injection.

17.5.1.3 ^{223}Ra Dichloride (Xofigo)

^{223}Ra dichloride, an alpha particle-emitting pharmaceutical is supplied as a clear, colorless, isotonic, and sterile solution to be administered intravenously with pH between 6 and 8. The drug product contains 1000 kBq or 27 μCi/mL of ^{223}Ra, corresponding to 0.53 ng Ra-223 at the reference date. Radium is present in the solution as a free divalent cation. Each vial contains 6 mL of solution (6000 kBq (162 μCi) radium-223 dichloride at the reference date). The inactive ingredients are 6.3 mg/mL sodium chloride USP (tonicity agent), 7.2 mg/mL sodium citrate USP (for pH adjustment), 0.2 mg/mL hydrochloric acid USP (for pH adjustment), and water for injection USP. The molecular weight of radium-223 dichloride, $^{223}RaCl_2$, is 293.9 g/mol. The SA of radium-223 is 1.9 MBq or 51.4 μCi/ng.

^{223}Ra has a half-life of 11.4 days. The six-stage decay of radium-223 to stable lead-207 occurs via short-lived daughters and is accompanied predominantly by alpha emissions. There are also beta and gamma emissions with different energies and emission probabilities. The fraction of energy emitted from radium-223 and its daughters as alpha-particles is 95.3% (5–7.5 MeV). The fraction emitted as beta-particles is 3.6% (average energies are 0.445 and 0.492 MeV), and the fraction emitted as gamma-radiation is 1.1% (energy range of 0.01–1.27 MeV).

Indications and Dosage: Xofigo is indicated for the treatment of patients with castration-resistant prostate cancer, symptomatic bone metastases, and no known visceral metastatic disease. The dose regimen of Xofigo is 50 kBq or 1.35 μCi/kg body weight, given at 4-week intervals for 6 injections.

Mechanism of action: ^{223}Ra mimics calcium and forms complexes with the bone mineral hydroxyapatite at areas of increased bone turnover, such as bone metastases. The high LET of alpha particles (80 keV/μm) leads to a high frequency of double-strand DNA breaks in adjacent cells, resulting in an anti-tumor effect on bone metastases. The alpha particle range <0.1 mm (less than 10 cell diameters) limits damage to the surrounding normal tissue.

Pharmacokinetics: After intravenous injection, ^{223}Ra is rapidly cleared from the blood and is distributed primarily into bone or is excreted into

the intestines. At 4 h, about 4% of the injected radioactivity remains in blood, decreasing to less than 1% at 24 h after the injection. At 4 h post-injection, the percentage of the radioactive dose present in bone and intestine is, approximately, 61% and 49%, respectively.

The efficacy and safety of Xofigo were evaluated in a double-blind, randomized, placebo-controlled phase 3 clinical trial of patients with CRPC with symptomatic bone metastases. Patients receiving the treatment with ^{223}Ra exhibited a 3.6-month prolonged survival time (PST) over the placebo group and a 5.8-month improved timeframe before the occurrence of a systematic skeletal-related event with a reduction of occurrence of spinal compression [55, 56]

17.5.2 Inorganic Chelate Complex

With the success of ^{99m}Tc bone imaging agents (such as MDP, HDP, EHDP) for targeting bone mineral hydroxyapatite, several β^- particle-emitting radiometals that can form chelate complexes were investigated for the development of radiopharmaceuticals for bone pain palliation. ^{153}Sm ($T½$ = 46.7 h, E_{mean} = 233 KeV), a trivalent lanthanide has a short half-life and low-energy beta particles and is a suitable alternative to Sr-90 which has a long half-life and high-energy beta emission. In addition, ^{153}Sm also has suitable γ photons (103 KeV) which make it suitable for imaging studies. ^{153}Sm forms a stable coordination complex with bisphosphonate analog EDTMP and ^{153}Sm-EDTMP was approved in 1997 for bone pain palliation. In the last two decades, several metal complexes were investigated as potential therapeutic agents for bone pain palliation such as ^{166}Ho-EDTMP, ^{177}Lu-EDTMP, ^{90}Y-EDTMP, ^{170}Tm-EDTMP, ^{117m}Sn-DTPA, and recently ^{177}Lu-DOTAZOL.

17.5.2.1 ^{153}Sm-Lexidronam (Quadramet®)

^{153}Sm-EDTMP (Quadramet®) (Fig. 17.10) was designed so that a tetraphosphonate chelator, EDTMP, a polydentate ligand, chelates ^{153}Sm 1:1 by forming four O-Sm bonds and two N-Sm bonds. EDTMP is structurally similar to bisphosphonates, which target bone due to their great

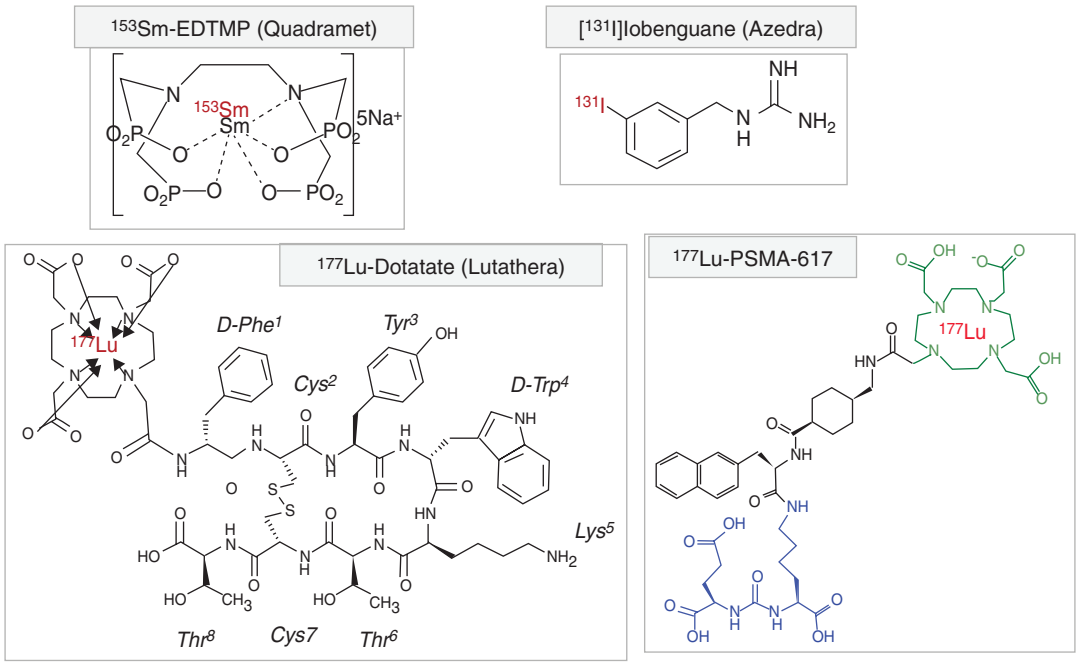

Fig. 17.10 Chemical structures of radiopharmaceuticals for TRT in clinical use

affinity for inorganic hydroxyapatite. The negatively charged ^{153}Sm-EDTMP readily chelates calcium cations and accumulates in the metastatic sites with increased metabolism and has higher calcium levels. QUADRAMET® is formulated as a sterile, non-pyrogenic, clear, colorless to light amber isotonic solution of samarium-153 lexidronam for intravenous administration [57].

Each milliliter contains 35 mg EDTMP·H_2O, 5.3 mg Ca[as $Ca(OH)_2$], 14.1 mg Na [as NaOH], equivalent to 44 mg Ca/Na EDTMP (anhydrous calc.), 5–46 μg samarium (specific activity of approximately 1.0–11.0 mCi/μg Sm), and 1850 ± 185 MBq (50 ± 5 mCi) of samarium-153 at calibration. The ionic formula is $^{153}Sm^{+3}[CH_2N(CH_2PO_3^{2-})_2]_2$ and the ionic formula weight is 581.1 Da (pentasodium form, 696). The pH of the solution is 7.0–8.5. QUADRAMET® is supplied frozen in single-dose glass vials containing 3 mL with 5550 MBq (150 mCi) of samarium-153 at calibration.

Indications: QUADRAMET® is indicated for relief of pain in patients with confirmed osteoblastic metastatic bone lesions that enhance on radionuclide bone scan.

Dosage and Administration: The recommended dose of QUADRAMET® is 1.0 mCi/kg, administered intravenously over a period of 1 min.

Clinical Pharmacology: QUADRAMET® has an affinity for bone and concentrates in areas of bone turnover in association with hydroxyapatite. It accumulates in osteoblastic lesions more than in normal bone with a lesion-to-normal bone ratio of approximately 5. The mechanism of action of QUADRAMET® in relieving the pain of bone metastases is not known. The greater the number of metastatic lesions, the more skeletal uptake of Sm-153 radioactivity. The total skeletal uptake of radioactivity is 65.5% ± 15.5% of the injected dose. Clearance of radioactivity from the blood demonstrated biexponential kinetics after intravenous injection in patients with a variety of primary cancers that were metastatic to bone. Over the first 30 min, the radioactivity in the blood decreased to 15 ± 8% of the injected dose. Less than 1% of the dose injected remained in the blood 5 h after injection. During the first 6 h, 34.5% (±15.5%) was excreted.

Drug Interactions: QUADRAMET® contains calcium and may be incompatible with solutions that contain molecules that can complex with and form calcium precipitates.

17.5.3 Particulate Carriers

Radiolabeled particles are generally used when the tumor is confined to a specific organ or an isolated body cavity. The goal is to obtain a uniformly distributed radiation dose within the cavity, while minimizing leakage into the rest of the body. In addition to stability, the most important characteristic of particulate carriers is their size because this dictates not only homogeneity of dose deposition but, also leakage from the treatment site. Two commercial preparations of ^{90}Y-labeled microspheres (20–60 μm), Theraspheres® and Sirspheres® are used for the treatment of hepatocellular carcinoma (HCC) and metastatic colorectal cancer [58]. Trans-arterial chemoembolization (TACE) involves administration of drugs intra-arterially for preferential localization in regions of tumor as majority of normal hepatic blood supply is via the portal vein and neo-angiogenic vessels are primarily connected to the hepatic artery. Following the release of the ^{90}Y-labeled microspheres in the hepatic artery via a microcatheter, the microspheres are permanently embedded in the terminal arterioles of the tumor. After the radio-embolization, the particles block the blood vessels and deliver the radiation dose locally. The ^{90}Y-labeled particles do not directly bind to cancer cells.

17.5.3.1 Theraspheres® Yttrium-90 Glass Microspheres

TheraSphere® consists of insoluble glass microspheres where yttrium-90 is an integral constituent of the glass. The mean sphere diameter ranges from 20 to 30 μm. Each milligram contains between 22,000 and 73,000 microspheres. TheraSphere® is supplied in 0.6 mL of sterile, pyrogen-free water contained in a 1.0 mL vial secured within a clear acrylic vial shield. TheraSphere® is available in 6 dose sizes: 3 GBq (81 mCi), 5 GBq (135 mCi), 7 GBq (189 mCi), 10 GBq (270 mCi), 15 GBq (405 mCi) and 20 GBq (540 mCi).

Indication: TheraSphere® is indicated for radiation treatment or as a neoadjuvant to surgery or transplantation in patients with unresectable hepatocellular carcinoma (HCC) who can have placement of appropriately positioned hepatic arterial catheters. The device is also indicated for HCC patients with partial or branch portal vein thrombosis/occlusion when clinical evaluation warrants the treatment. Theraspheres® has been used in the clinic for the last 8 years under a humanitarian device exemption (HDE) but, in March of 2021, Theraspheres® formally received FDA approval as a device.

Mechanism: Following embolization of the yttrium-90 glass microspheres in tumorous liver tissue, the beta radiation emitted provides a therapeutic effect [11, 27, 29, 59, 60]. The microspheres are delivered into the liver tumor through a catheter placed into the hepatic artery that supplies blood to the tumor. The microspheres, being unable to pass through the vasculature of the liver due to arteriolar capillary blockade, are trapped in the tumor and exert a local radiotherapeutic effect with some concurrent damage to surrounding normal liver tissue.

17.5.3.2 SirSpheres® Microspheres (Yttrium-90 Microspheres)

SIR-Spheres® microspheres consist of biocompatible microspheres containing yttrium-90 with a size between 20 and 60 μm in diameter. The average number of particles implanted is 30–60 × 10^6. SIR-Spheres microspheres are provided in a vial with water for injection. Each vial contains 3 GBq of yttrium-90 ±10% (at the time of calibration) in a total of 5 cc water for injection. Each vial contains 40–80 million microspheres. SIR-Spheres® microspheres are a permanent implant.

Indications for Use: SIR-Spheres® microspheres are indicated for the treatment of unresectable metastatic liver tumors from primary colorectal cancer with adjuvant intra-hepatic artery chemotherapy (IHAC) of FUDR (Floxuridine).

17.5.4 Small Organic Molecules

MIBG was originally designed and developed in 1980 for imaging adrenal medulla [61]. MIBG, an analog of norepinephrine (Fig. 17.10) was synthesized by linking the benzyl portion of bretylium with the guanidine group of guanethidine. In 1994, [^{131}I]MIBG also known as iobenguane sulfate I-131 intravenous (low specific activity *(LSA)* formulation), received FDA approval as an imaging agent for the localization of specific sites of pheochromocytomas and neuroblastomas (Pharmalucence 2008). In 2008, [^{123}I]MIBG or iobenguane I-123 injection was also approved by the FDA as a tumor imaging agent (Adreview; GE Healthcare).

In 2018, the FDA approved high specific activity iobenguane I-131(Azedra™) for the treatment of paragangliomas and pheochromocytomas. It is also used for the treatment of pediatric patients with neuroblastoma [62]. The uptake of MIBG into the neuroendocrine cell is by two mechanisms—active and passive [63]. The active transport or the uptake-1 system is the dominant method of transport of MIBG into the cell. This is an active, sodium and energy-dependent amine uptake mechanism in the cell membrane of the sympathomedullary tissues. Within the cell, it is actively transported into the storage granules by an energy-dependent transport mechanism via vesicular monoamine transporters 1 and 2. This accumulation of MIBG in these neurosecretory granules forms the basis for imaging and therapy with ^{123}I/^{131}I-labeled MIBG [62]. Small amount of MIBG is also present in the cytoplasm. The other mechanism is a passive diffusion of MIBG into the cells. The active uptake is more efficient and specific than the passive uptake.

17.5.4.1 AZEDRA® (Iobenguane I 131) Injection

The drug substance iobenguane I 131, also described as mIBG (Fig. 17.9), has a molecular weight of 279.1 Da. AZEDRA 555 MBq/mL (15 mCi/mL) injection is a sterile, clear, colorless to pale yellow solution. Each single-dose vial contains iobenguane (0.006 mg/mL), sodium ascorbate (58 mg/mL) and sodium gentisate (23 mg/mL) in water for Injection, USP. The pH range of the solution is 4.5–5.5, with a specific activity of ~2500 mCi/mg (92,500 MBq/mg) [64].

Indications and Usage: AZEDRA is indicated for the treatment of adult and pediatric patients

12 years and older with iobenguane scan positive, unresectable, locally advanced, or metastatic pheochromocytoma or paraganglioma who require systemic anticancer therapy.

Dosage and Administration: Recommended dosimetric dose: patients weighing more than 50 kg: 185–222 MBq (5–6 mCi); patients weighing 50 kg or less: 3.7 MBq/kg (0.1 mCi/kg); Recommended therapeutic dose: patients weighing >62.5 kg: 18.5 GBq (500 mCi) and patients weighing 62.5 kg or less: 0.296 GBq/kg (8 mCi/kg). Administer 2 therapeutic doses 90 days apart. As needed, adjust the therapeutic doses based on radiation dose estimate results from dosimetry study.

Mechanism of Action: Iobenguane is similar in structure to the neurotransmitter norepinephrine (NE) and is subject to the same uptake and accumulation pathways as NE. Iobenguane is taken up by the NE transporter in adrenergic nerve terminals and accumulates in adrenergically innervated tissues, such as the heart, lungs, adrenal medulla, salivary glands, liver, and spleen, as well as tumors of neural crest origin. Pheochromocytoma and paraganglioma (PPGL) are tumors of neural crest origin that express high levels of the NE transporter on their cell surfaces.

Pharmacodynamics: The effect of AZEDRA on the QTc interval was evaluated in 74 patients with unresectable pheochromocytoma or paraganglioma. At the recommended therapeutic dosage, no large mean increases from baseline in the QTc interval (i.e., >20 ms) were detected.

Pharmacokinetics: Iobenguane I 131 is primarily eliminated renally with cumulative excretion of 50 ± 10% within 24 h and 80 ± 10% within 120 h following AZEDRA administration. Unchanged I 131 accounted for an average of 94% and 93% radioactivity excreted in urine collected during 0–6 and 6–24-h post-dose, respectively. Minor metabolites detected in some patients included free I 131, quantifiable in 55% of 11 patients in Study IB11, as well as meta-iodohippuric acid (MIHA) and meta-iodobenzyl bisguanidine (MMIBG) quantifiable in one patient each.

Drug Interactions: Based on the mechanism of action of iobenguane, drugs that reduce catecholamine uptake or that deplete catecholamine stores may interfere with iobenguane uptake into cells and, therefore, interfere with dosimetry calculations or the efficacy of AZEDRA. Discontinue drugs that reduce catecholamine uptake or deplete catecholamine stores for at least five half-lives before administration of either the dosimetry or a therapeutic dose of AZEDRA. Do not administer these drugs until at least 7 days after each AZEDRA dose.

17.5.5 Regulatory Peptides Hormone Analogs

Peptides are formed when two or more amino acids are condensed together with the formation of a secondary amide bond, the so-called peptide bond or peptide unit. Most of the drawbacks of mAbs can be eliminated by using biomolecules like peptides [65]. Peptides are quickly cleared from the blood circulation by liver and kidney. In addition, the pharmacodynamic properties of peptides can be modulated by different synthetic modification and stabilization approaches. Peptides are generally considered safe since they feature low immunogenicity and produce non-toxic metabolites. Since peptides are small molecules, they can easily penetrate into the solid tumors unlike mAbs.

Various peptides, peptide receptors, and the corresponding eligible target-related tumors are summarized in Table 17.11. The overexpression of peptide receptors on tumor cells leads to the development of radiolabeled peptides for diagnosis and therapy [66, 67]. It has been demonstrated that only tumors expressing a high density of receptors can be selected for targeted therapy. A tumor-to-normal-cell expression ratio of 3:1 or higher is usually desired. Secondly, the amounts of overexpressed receptors must be sufficient to ensure drug delivery in appropriate amounts to obtain the desired therapeutic effect. Since peptide agonists are quickly metabolized (or inactivated) by amino peptidases, following binding to receptors, peptide radiopharmaceuticals are generally developed using chemically modified peptide analogs that may have greater affinity for the receptor but, block the receptor function.

17.5.5.1 Somatostatin Receptors

The most well-studied cell surface receptor is the somatostatin receptor (SSTR) family, which is comprised of five members (SSTR1-5). Their natural ligand is the disulfide-cyclized oligopeptide somatostatin (SST), which occurs in two isoforms SST-14 and SST-28. Human SST receptors (SSTR1-SSTR5) have been identified in most of the neuroendocrine tumors, small cell lung cancers, and medullary thyroid carcinoma, expressing high densities of SSTRs. The expression of SSTR subtypes in human tumor tissues, however, seems to vary among different tumor types. Although various SS receptor subtypes are expressed in tumors, SSTR2 is the predominant receptor subtype expressed in NETs. Since SST is degraded rapidly in vivo, octreotide (Sandostatin) was developed as a therapeutic agent. It is the presence of SSTR2 as well as its density which provides the molecular basis for several radiolabeled SS analogs (Fig. 17.9) that were developed for diagnosis and peptide receptor therapy (PRT). ^{111}In-DTPA-octreotide (Octreoscan) was the first peptide approved as an imaging agent in 1993.

The acronyms PRS (peptide receptor scintigraphy) and PRRT (peptide receptor radionuclide therapy) were originally coined in the 1980s by the investigators at the Erasmus University Medical Center, Rotterdam, in the Netherlands. Following the development of DOTA conjugated octreotide analogs (DOTATOC and DOTATATE) in the early 1990s, the first clinical results with ^{90}Y-DOTATOC demonstrated the potential therapeutic effectiveness of PRRT in patients with NETs [68]. Subsequently, the efficacy and safety of ^{177}Lu-DOTATOC and ^{177}Lu-DOTATATE were investigated extensively in several multicenter clinical trials. The FDA approval of ^{177}Lu-DOTATATE (Lutathera®) in 2017, a peptide radiopharmaceutical specific for SSTR, is clinically indicated for the treatment of neuroendocrine tumors started a new wave in the development of peptide-based radiopharmaceuticals for TRT.

17.5.5.2 Lutathera® (^{177}Lu-Dotatate) Injection

Lutathera® is a radiolabeled somatostatin analog [69]. The drug substance ^{177}Lu-dotatate is a cyclic peptide, Tyr^3-octreotide linked with the covalently bound chelator DOTA (1,4,7,10-tetraazacyclododecane-1,4,7,10-tetraacetic acid) and labeled with ^{177}Lu radionuclide. The molecular weight is 1609.6 Da, and the structural formula is as shown in Fig. 17.10. Lutathera® 370 MBq/mL (10 mCi/mL) Injection is a sterile, clear, colorless to slightly yellow solution for intravenous use. Each single-dose vial contains acetic acid (0.48 mg/mL), sodium acetate (0.66 mg/mL), gentisic acid (0.63 mg/mL), sodium hydroxide (0.65 mg/mL), ascorbic acid (2.8 mg/mL), diethylene triamine pentaacetic acid (0.05 mg/mL), sodium chloride (6.85 mg/mL), and water for injection (ad 1 mL). The pH range of the solution is 4.5–6.

Indications and Usage: Lurathera® is indicated for the treatment of somatostatin receptor-positive gastroenteropancreatic neuroendocrine tumors (GEP-NETs), including foregut, midgut, and hindgut neuroendocrine tumors in adults.

Dosage and Administration: The recommended Lutathera dose is 7.4 GBq (200 mCi) every 8 weeks for a total of 4 doses. Premedication and Concomitant Medications: (a) Before initiating Lutathera® therapy, discontinue long-acting somatostatin analogs for at least 4 weeks. Administer short-acting octreotide, as needed, and discontinue at least 24 h prior to therapy dose. (b) Administer long-acting octreotide 30 mg intramuscularly between 4 and 24 h after each therapy dose. Do not administer long-acting octreotide within 4 weeks of each subsequent Lutathera® dose. (c) Initiate an intravenous amino acid solution (1.5–2.2 L) containing L-lysine (20–25 g) and L-arginine (20–25 g) 30 min before administering Lutathera and continued during, and for at least 3 h after Lutathera infusion.

Pharmacokinetics: Within 4 h after administration, Lu-177 dotatate distributes in kidneys, tumor lesions, liver, spleen, and, in some patients, pituitary gland and thyroid. The co-administration of amino acids reduced the median radiation dose to the kidneys by 47%. The effective blood elimi-

nation half-life is 3.5 ± 1.4 h and the mean terminal blood half-life is 71 ± 28 h. Lu-177 dotatate is primarily eliminated renally with cumulative excretion of 44% within 5 h, 58% within 24 h, and 65% within 48 h following Lutathera® administration.

Mechanism of Action: Lutathera® binds to somatostatin receptors with highest affinity for subtype 2 receptors (SSRT2). Upon binding to somatostatin receptor-expressing cells, including malignant somatostatin receptor-positive tumors, the compound is internalized. The β^- particles from Lu-177 induce cellular damage by formation of free radicals in somatostatin receptor-positive cells and in neighboring cells.

Drug Interactions: Somatostatin and its analogs competitively bind to somatostatin receptors and may interfere with the efficacy of Lutathera®. Discontinue long-acting somatostatin analogs at least 4 weeks and short-acting octreotide at least 24 h prior to each Lutathera® dose.

17.5.5.3 Other Peptide Receptors

Many other peptide receptors have been identified and are known to be overexpressed in several different cancers (Table 17.11). Radiolabeled peptides are being developed to target-specific receptors for Glucagon-like peptide 1 receptor (GLP-IR), Gastrin or cholecystokinin-2 receptor (CCK2R), Neurotensin receptor 1 (NTR1), Chemokine receptor-4 (CXCR), Vasoactive intestinal peptide (VIP), neurotensin (NT) receptor, substance-P, and neuropeptide-Y. Preclinical studies and phase I/II clinical studies demonstrated the potential of several radiolabeled peptides for both imaging studies, and for targeted radionuclide therapy.

17.5.6 Monoclonal Antibodies

An antibody (Ab), also known as an immunoglobulin (Ig) is a large protein used by the immune system to identify and neutralize foreign objects such as pathogenic bacteria and viruses. The antibody recognizes a unique molecule of the pathogen, called an antigen. The antibody molecule contains a paratope (antigen binding segment) that is specific for epitope (Ab binding segment) on an antigen. Antibody and antigen interact by spatial complementarity (like lock and key). The binding between antibody and antigen is reversible and, as a result, it is possible for an antibody to cross-react with different antigens of different relative affinities. Polyclonal antibodies (pAbs) are a heterogeneous mixture produced by different B cell clones in the body but, bind to many different epitopes of a single antigen. In contrast, mAbs are generated by identical B cells which are clones from a single parent cell. This means that the mAb binds to a single epitope and is monovalent. Georges Köhler and César Milstein invented the technology of producing mAbs [70] and started the modern era of antibody-based pharmaceuticals.

Antibodies are large glycoproteins and their basic structure is composed of two heavy and two light chains in the shape of a Y. At each tip of the Y lies the fragment antigen-binding (Fab) portion of the antibody which is responsible for recognition of the specific antigen. The fragment crystallizable (Fc) region located at the base of the Y structure mediates interactions between the antibody and other members of the immune system. Antibody Fc regions are recognized by Fc receptors (FcRs) found on a wide range of immune cells. IgG is the most often form used in antibody therapy due to the fact that IgGs interact with their associated type of Fc-receptor found on natural killer (NK) cells as well as neutrophils, monocytes, dendritic cells, and eosinophils to mediate specialized functions such as antibody-dependent cellular cytotoxicity (ADCC) and complement-dependent cytotoxicity (CDC). Intact mAbs have a long residence time in humans, ranging from a few days to weeks, which results in optimal tumor-to-non-tumor ratios at 2–4 days post-injection. In contrast, mAb fragments have a much faster blood clearance and, as a result, optimal tumor-to-nontumor ratios can be obtained at earlier time points. However, the absolute tumor uptake may be much lower compared to intact mAbs. Around the world, more than 600 therapeutic mAbs have been studied in clinical trials, and close to 80 therapeutic mAbs have been approved by the FDA for different diseases including cancer [71].

17.5.6.1 Radioimmunotherapy (RIT)

RIT exploits the ability of radiolabeled antibody conjugates (RACs) to target tumors in an antigen-specific manner for selective delivery of therapeutic radionuclide and localized release of cytotoxic ionizing but, non-penetrating radiations, such as α *particles and* β^- particles. The efficacy of RIT, however, depends on the type and size of cancer tissue and the choice of radionuclide, half-life, type of particle emission, kinetic energy, and range in tissue. The first use of radiolabeled antibody to treat cancer was performed in the 1950s by Dr. Beierwalters at the University of Michigan, USA, who used ^{131}I-tagged antibodies made in rabbits against patient's own neoplastic tissue [59].

After several decades of intense investigation with radiolabeled antibodies, only six radiolabeled antibodies have gained FDA approval for use in clinical oncology, including four immunodiagnostic agents and two targeted radioimmunotherapeutic agents (Table 17.2). As of December 2021, more than 30 mAbs have been approved for the treatment of cancer. RIT with antibodies, however, was not clinically successful except in hematological malignancies. Combining mAbs with therapeutic radionuclides was first studied in hematologic malignancies based on the rationale that these cancers are the most radiosensitive tumors compared to solid tumors [72, 73]. The FDA's approvals of 2 radiolabeled anti-CD20 mAbs, ^{90}Y-labeled Zevalin® (ibritumomab tiuxetan) in 2002 and ^{131}I-labeled Bexxar® in 2003 for the treatment of NHL were landmark events in the developmental history of TRT and RIT. Both these ^{90}Y- and ^{131}I-labeled anti-B1 mAbs produce overall response rates (ORR, 60–80%) and complete response rates (CRR, 15–40%) in relapsed NHL longer than the naked antibodies, such as rituximab [73].

17.5.6.2 ZEVALIN® (Ibritumomab Tiuxetan) Injection

Zevalin (ibritumomab tiuxetan) is the immunoconjugate resulting from a stable thiourea covalent bond between the mAb ibritumomab and the linker-chelator tiuxetan [*N*-[2-bis(carboxymethyl) amino]-3-(p-isothiocyanatophenyl)-propyl]-[*N*-[2-bis(carboxymethyl)amino]-2-(methyl)-ethyl] glycine. This linker-chelator provides a high affinity, conformationally restricted chelation site for ^{111}In or ^{90}Y. The approximate molecular weight of ibritumomab tiuxetan is 148,000 Da. The antibody moiety of Zevalin is ibritumomab, a murine IgG_I kappa mAb directed against the CD20 antigen. Ibritumomab tiuxetan is a clear, colorless, sterile, pyrogen-free, preservative-free solution that may contain translucent particles. Each single-use vial includes 3.2 mg of ibritumomab tiuxetan in 2 mL of 0.9% sodium chloride.

Indications and Usage: Zevalin is indicated for the treatment of relapsed or refractory, low-grade, or follicular B-cell non-Hodgkin's lymphoma (NHL). Zevalin is also indicated for the treatment of previously untreated follicular NHL in patients who achieve a partial, or complete response to first-line chemotherapy.

Recommended Doses: Dose for biodistribution imaging study: 5 mCi of ^{111}In-Zevalin; Therapeutic dose: 0.4 mCi/kg (14.8 MBq/kg) for patients with normal platelet count; 0.3 mCi/kg (11.1 MBq/kg) in relapsed or refractory patients with platelet count of 10,000–149,000 cells/mm. Prior to the administration of the dosimetric or therapeutic dose, first administer rituximab 250 mg/m^2 intravenously at an initial rate of 50 mg/h. In the absence of infusion reactions, escalate the infusion rate in 50 mg/h increments every 30 min to a maximum of 400 mg/h. The dose of ^{90}Y-Zevalin should not exceed 32.0 mCi (1184 MBq). The specific activity of ^{90}Y-Zevalin is around 20 mCi/mg of antibody. ^{90}Y-Zevalin should not be injected into patients with altered biodistribution as determined by imaging with ^{111}In-Zevalin

Mechanism of Action: Ibritumomab tiuxetan binds specifically to the CD20 antigen (human B-lymphocyte-restricted differentiation antigen, Bp35). The apparent affinity (K_D) of ibritumomab tiuxetan for the CD20 antigen ranges between approximately 14 and 18 nM. The CD20 antigen is expressed on pre-B and mature B lymphocytes and on >90% of B-cell non-Hodgkin's lymphomas (NHL). The CD20 antigen is not shed from the cell surface and does not internalize upon antibody binding.

Pharmacodynamics: Administration of the Zevalin therapeutic regimen resulted in sustained depletion of circulating B cells. At 4 weeks, the median number of circulating B cells was zero. B-cell recovery began at approximately 12 weeks following treatment, and the median level of B cells was within the normal range by 9 months after treatment.

Pharmacokinetics: With ^{111}In-Zevalin imaging studies, only 18% of known sites of disease were imaged when ^{111}In-Zevalin was administered alone without unlabeled ibritumomab. However, when preceded by unlabeled ibritumomab (2.5 mg/kg), ^{111}In-Zevalin detected 92% of known disease sites. With ^{90}Y-Zevalin therapeutic dose administration, the mean effective half-life for Y-90 activity in blood was 30 h and the mean area under the fraction of injected activity (FIA) vs. time curve in blood was 39 h. Over 7 days, a median of 7.2% of the injected activity was excreted in urine.

17.5.6.3 BEXXAR® (Tositumomab and Iodine I 131 Tositumomab) Injection

The BEXXAR® therapeutic regimen is composed of the mAb tositumomab, and the radiolabeled mAb, ^{131}I-tositumomab. Tositumomab is a murine IgG_{2a} lambda mAb directed against the CD20 antigen, produced in mammalian cells. The approximate molecular weight of tositumomab is 150 kDa. Tositumomab is supplied as a sterile, pyrogen-free, clear to opalescent, colorless to slightly yellow, preservative-free solution that must be diluted before intravenous administration. The formulation contains 100 mg/mL maltose, 8.5 mg/mL sodium chloride, 1 mg/mL phosphate, 1 mg/mL potassium hydroxide, and water for injection. The pH is approximately 7.2.

Tositumomab is covalently linked to ^{131}I and is supplied as a sterile, clear, preservative-free liquid. The drug product formulation contains 0.9–1.3 mg/mL ascorbic acid, 1–2 mg/mL maltose (dosimetric dose) or 9–15 552 mg/mL maltose (therapeutic dose), 4.4–6.6% (w/v) povidone, and 8.5–9.5 mg/mL sodium 553 chloride. The pH is approximately 7.0. I-131 tositumomab is supplied as a sterile, clear, preservative-free liquid. The formulation for I-131 tositumomab contains 0.9–1.3 mg/mL ascorbic acid, 1–2 mg/mL maltose (dosimetric dose), or 9–15 mg/mL maltose (therapeutic dose), 4.4–6.6% (w/v) povidone, and 8.5–9.5 mg/mL sodium chloride. The pH is approximately 7.0.

For dosimetry studies, ^{131}I-tositumomab is supplied 12–18 mCi/vial (NLT 0.61 mCi/mL and 0.1 mg/mL). For therapy, ^{131}I-tositumomab is supplied 112–168 mCi/vial (NLT 5.6 mCi/mL and 1.1 mg/mL).

Dosage and Administration: The therapeutic regimen consists of two separate components (tositumomab and ^{131}I-tositumomab) administered in two separate steps (dosimetric dose and therapeutic dose) separated by 7–14 days. For dosimetry study, 450 mg of Tositumomab followed by 5 mCi of ^{131}I-Tositumomab (450 mg) and for therapy, 450 mg of Tositumomab followed by ^{131}I-Tositumomab therapy dose (the amount of ^{131}I activity to deliver 65–75 cGy depending on the platelet counts and total body residence time determined following dosimetric dose).

Mechanism of Action: Tositumomab binds specifically to an epitope within the extracellular domain of the CD20 molecule, expressed on normal B lymphocytes and on B-cell NHLs. non-Hodgkin's lymphomas. In addition to cell death mediated by the radioisotope, other possible mechanisms of action include ADCC, CDC, and CD20-mediated apoptosis.

Pharmacodynamics: The administration of the BEXXAR® therapeutic regimen resulted in sustained depletion of circulating CD20-positive cells (normal and malignant). At 7 weeks following treatment, the median number of circulating CD20-positive cells was zero with recovery beginning at approximately 12 weeks.

Pharmacokinetics: Prior administration of 475 mg of naked antibody decreased splenic targeting and increased the terminal half-life of the ^{131}I-tositumomab. Patient-specific dosing, based on total body clearance, provided a consistent radiation dose despite variable pharmacokinetics, by allowing each patient's administered activity to be adjusted for individual patient variables. The median total body effective half-life, in

patients with NHL was 67 h. Five days following the radiolabeled dose, the whole-body clearance was 67% of the injected dose. Due to in vivo dehalogenation, ^{131}I-tositumomab is not stable in vivo and the free I-131 activity is excreted in the urine.

17.6 Prostate Specific Membrane Antigen (PSMA)

In 1987, prostate-specific membrane antigen (PSMA) was discovered as a novel antigenic marker in prostate cancer cells and in the serum of prostate cancer patients. In the brain, PSMA is also known as *N*-acetyl-L-aspartyl-L-glutamate peptidase I (*NAALADase I*) or *N*-acetyl-aspartyl-glutamate (*NAAG) peptidase* [74]. PSMA is considered to be the most well-established target antigen in prostate cancer, since it is highly and specifically expressed at all tumor stages on the surface of prostate tumor cells compared with normal or hyperplastic prostates [75, 76]. PSMA is a class II transmembrane glycoprotein with a unique 3-part structure: a short N-terminal cytoplasmic tail, a single membrane-spanning helix, and an extracellular part. The bulk of PSMA protein is the extracellular part.

In 1997, Bander and his colleagues at Weill Cornell Medicine in New York reported the development J591 mAb to the extracellular domain of PSMA on viable tumor cells [77, 78]. J591 mAb targets the extracellular portion of PSMA and therefore, binds to the viable tumor cells [77]. In the last 20 years, several clinical studies documented the therapeutic potential of ^{90}Y-, ^{177}Lu-, and ^{225}Ac-labeled DOTA-huJ591 for RIT of mCRPC [79–81].

17.6.1 PSMA Inhibitors

The enzyme activity of PSMA includes *NAALADase 1*. In the brain, PSMA hydrolyzes the *N*-acetyl-L-aspartyl-L-glutamate (NAAG) substrate to yield aspartate and glutamate. Studies of the *NAALADase* enzyme structure have revealed an active site containing two zinc cations (Zn^{++}) participating in the NAAG binding, called the "*NAAG binding pocket*", which is also the site for the binding of PSMA inhibitors [60]. The discovery of small molecule peptide PSMA inhibitors made it possible for the development of both diagnostic and therapeutic peptide radiopharmaceuticals. PSMA enzyme inhibitors mimic the structure of the substrate (NAAG), bind to PSMA, and reduce the ability of the enzyme to convert the substrate NAAG into aspartate and glutamate (Pastarino et al. 2020). The clinical success of radiolabeled PSMA inhibitors is based on a small motif binding to the catalytic NAAG hydrolyzing site in the PSMA molecule. This class of inhibitors contains a urea bond (−NH-CO-NH-) formed by the conjugation of two amino acids (Glu and Asp). Several groups have reported on the development of small-molecule inhibitors of PSMA comprising two amino acids joined through their NH_2 groups by a urea linkage (glutamate urea heterodimers) [81]. In the last 2 years, two radiolabeled PSMA inhibitors, ^{68}Ga-PSMA-11 and [^{18}F]DCFPyL have already been approved by the FDA for PET imaging studies of prostate cancer [83, 84].

17.6.1.1 ^{177}Lu-PSMA-617

To develop radiopharmaceuticals for TRT, two PSMA inhibitors, PSMA-617 and PSMA I&T were developed at the German Cancer Research Centre (GCRC) in Heidelberg, Germany based on Glu-Urea-Lys pharmacophore and DOTA or DOTAGA chelators respectively [85]. ^{177}Lu-PSMA-617 (Fig. 17.10) was quickly used as a therapeutic ligand because it has higher tumor uptake at later time points, lower spleen uptake, and highly efficient clearance from the kidneys [86]. Clinical studies have also evaluated the potential of ^{68}Ga-PSMA I&T for the detection of primary prostate cancer before prostatectomy [82].

The first clinical experience with ^{177}Lu-PSMA-617 targeted therapy in patients with advanced mCRPC demonstrated that ^{177}Lu-PSMA-617 is a promising new option for therapy of mCRPC [87]. Subsequently, two major clinical studies evaluated the safety and

efficacy of ^{177}Lu-PSMA-617 therapy in patients with mCRPC. A randomized, multi-center open-label phase 2 trial (TheraP trial) compared the efficacy of ^{177}Lu-PSMA-617 with cabazitaxel in patients with mCRPC [88]. The study results showed that ^{177}Lu-PSMA-617 treatment, compared to cabazitaxel, led to a higher PSA response and fewer grade 3 or 4 adverse events.

The VISION trial (Funded by Endocyte, a Novartis company) evaluated the advantages of ^{177}Lu-PSMA-617 over best supportive care in improving the overall survival (OS) and image-based progression-free survival (PFS) in patients with progressive mCRPC [89]. Five hundred and fifty-one patients were allotted to the ^{177}Lu-PSMA-617 group (who received 7.4 GBq of ^{177}Lu-PSMA-617 every 6 weeks in 4–6 cycles), while 280 patients were in the standard of care (SOC) group. The results of the study showed that the median PFS was significantly longer among patients in the ^{177}Lu-PSMA-617 arm at 8.7 months compared with 3.4 months in patients in the SOC-alone arm. There was a significant improvement in the OS in the patients who received ^{177}Lu-PSMA-617 compared to standard care alone (15.3 months vs. 11.3 months). Also, approximately 46% (vs. 7.1% in control group) of the patients had >50% reduction, and >33% (vs. 2% in control group) of the patients had >80% reduction in the PSA levels (SOC). The FDA granted priority review for the NDA for^{177}Lu-PSMA-617 and approved in 2022 to treat patients with metastatic castration-resistant prostate cancer (mCRPC) who have previously received androgen-receptor pathway and taxane-based chemotherapy.

The successful completion of phase III clinical trial of ^{177}Lu-PSMA-617 (VISION Trial) and fast approval by FDA in the treatment of mCRPC may also help advance the development of several new peptide or protein based radiopharmaceuticals for TRT.

References

1. Troy DB, Beringer P, editors. Remington: the science and practice of pharmacy. 21st ed. Philadelphia: Lippincott Williams & Wilkins; 2006.
2. Christiansen JA, Hevesy GD, Lomholt S. Recherches, par une methode radiochimique, sur la circulationdu bismuth dans l'organisme. Compt Rend. 1924;178:1324.
3. Lomholt S. Notes on the pharmacology of bismuth, with reference to its employment in the therapy of syphilis. Br J Vener Dis. 1925;1(1):50–7.
4. Seidlin SM, Marinelli LD, Oshry E. Radioactive iodine therapy: effect on functioning metastases of adenocarcinoma of the thyroid. JAMA. 1946;32(14):838–47.
5. Vallabhajosula S. The chemistry of therapeutic radiopharmaceuticals. In: Aktolun C, Goldsmith SJ, editors. Nuclear medicine therapy: principles and clinical applications. New York: Springer Science+Business Media; 2013.
6. Chakravarty R, Chakraborty S. A review of advances in the last decade on targeted cancer therapy using ^{177}Lu: focusing on ^{177}Lu produced by the direct neutron activation route. Am J Nucl Med Mol Imaging. 2021;11(6):443–75.
7. Sgouros G, Bodei L, McDevitt MR, Nedrow JR. Radiopharmaceutical therapy in cancer: clinical advances and challenges. Nat Rev Drug Discov. 2020;19:589.
8. O'Donoghue JA, Bardiès M, Wheldon TE. Relationships between tumor size and curability for uniformly targeted therapy with beta-emitting radionuclides. J Nucl Med. 1995;36(10):1902–9.
9. IAEA-RRS-2. Production of long-lived parent radionuclides for generators: ^{68}Ge, ^{82}Sr, ^{90}Sr and ^{188}W. Vienna: International Atomic Energy Agency; 2010.
10. IAEA TRS-470. Therapeutic radionuclide generators: ^{90}Sr/^{90}Y AND ^{188}W/^{188}Re generators. Vienna: International Atomic Energy Agency; 2009.
11. Banerjee S, Pillai MRA, Knapp FF. Lutetium-177 therapeutic radiopharmaceuticals: linking chemistry, radiochemistry, and practical applications. Chem Rev. 2015;115(8):2934–74.
12. Medvedev DG, Mausner LF, Meinken GE, et al. Development of a large-scale production of Cu-67 from Zn-68 at the high energy proton accelerator: closing the Zn-68 cycle. Appl Radiat Isot. 2012;70:423–9.
13. Ehst DA, Smith NA, Bowers DL, Makarashvili V. Copper-67 production on electron linacs—photonuclear technology development. AIP Conf Proc. 2012;1509:157–61.
14. Mamtimin M, Harmon F, Starovoitova VN. Sc-47 production from titanium targets using electron linacs. Appl Radiat Isot. 2015;102:1–4.
15. Mikolajczak R, Huclier-Markai S, Alliot C, et al. Production of scandium radionuclides for theranostic applications: towards standardization of quality requirements. EJNMMI Radiopharm Chem. 2021;6:19.
16. Rotsch DA, Brown MA, Nolen JA, et al. Electron linear accelerator production and purification of scandium-47 from titanium dioxide targets. Appl Radiat Isot. 2018;2018(131):77–82.

17. Lehenberger S, Barkhausen C, Susan Cohrs S, et al. The low-energy β⁻ and electron emitter ^{161}Tb as an alternative to ^{177}Lu for targeted radionuclide therapy. Nucl Med Biol. 2011;38(6):917–24.
18. Gracheva N, Müller C, Talip Z, et al. Production and characterization of no-carrier-added ^{161}Tb as an alternative to the clinically applied ^{177}Lu for radionuclide therapy EJNMMI. Radiopharm Chem. 2019;4:12.
19. Nicholas AL, Aldama DL, Verpelli M. Handbook of nuclear data for safeguards. International Atomic Energy Agency. 2008. IAEA-INDC (NDS)-0534.
20. Stevenson NR, St. George G, Simon J, Srivastava SC. Methods of producing high specific activity Sn-117m with commercial cyclotrons. J Radioanal Nucl Chem. 2015;305(1):99–108. https://doi.org/10.1007/s10967-015-4031-7.
21. IAEA-TRS-468. Cyclotron produced radionuclides: physical characteristics and production methods. Vienna: International Atomic Energy Agency; 2009.
22. Balkin ER, Cutler CS. Scale-up of high specific activity ^{186g}Re production using graphite-encased thick ^{186}W targets and demonstration of an efficient target recycling process. Radiochimica Acta. 2017;105:1071–81.
23. Klaassen NJM, Arntz MJ, Arranja AG, et al. The various therapeutic applications of the medical isotope holmium-166: a narrative review. EJNMMI Radiopharm Chem. 2019;4(1):19.
24. Kozempel J, Mokhodoeva O, Vlk M. Progress in targeted alpha-particle therapy. What we learned about recoils release from in vivo generators. Molecules. 2018;23:581.
25. Tinganelli W, Ma NY, Von Neubeck C, et al. Influence of acute hypoxia and radiation quality on cell survival. J Radiat Res. 2013;54(Suppl 1):23–30.
26. Eychenne R, Chérel M, Haddad F, et al. Overview of the most promising radionuclides for targeted alpha therapy: the "hopeful eight". Pharmaceutics. 2021;13:906.
27. Apostolidis C, Molinet R, McGinley J, et al. Cyclotron production of Ac-225 for targeted alpha therapy. Appl Radiat Isot. 2005;62:383–7.
28. IAEA Report. IAEA report on joint IAEA-JRC workshop "Supply of Actinium-225". Vienna: International Atomic Energy Agency; 2018.
29. Ahenkorah S, Cassells I, Deroose CM, et al. Bismuth-213 for targeted radionuclide therapy: from atom to bedside. Pharmaceutics. 2021;13:599.
30. Bertrand A, Legras B, Martin J. The use of radium-224 in the treatment of ankylosing spondylitis and rheumatoid synovitis. Health Phys. 1978;1:57–60.
31. Moiseeva AN, Aliev RA, Unezhev VN, et al. Cross section measurements of 151Eu(3He,5n) reaction: new opportunities for medical alpha emitter 149Tb production. Sci Rep. 2020;10:1–7.
32. Cavaier F, Haddad F, Sounalet T, et al. Terbium radionuclides for theranostics applications: a focus on MEDICIS-PROMEDR. Phys Procedia. 2017;90:157–63.
33. Ku A, Facca VJ, Cai Z, Reilly RM. Auger electrons for cancer therapy—a review. EJNMMI Radiopharm Chem. 2019;2019(4):27–63.
34. Howell RW, Rao DV, Hou D-Y, Narra VR, Sastry KSR. The question of relative biological effectiveness and quality factor for Auger emitters incorporated into proliferating mammalian cells. Radiat Res. 1991;128:282–92.
35. Edem PE, Fonslet J, Kjær A, et al. In vivo radionuclide generators for diagnostics and therapy bioinorganic chemistry and applications. Bioinorg Chem Appl. 2016;2016:6148357.
36. Mausner L, Straub R, Srivastava S. The in vivo generator for radioimmunotherapy. J Labell Comp Radiopharm. 1989;26(1–12):498–500.
37. McDevitt MR, Ma D, Lai L, et al. Tumor therapy with targeted atomic nanogenerators. Science. 2001;294:1537–40.
38. Kruijff RM, Wolterbeek HT, Denkova AG. A critical review of alpha radionuclide therapy—how to deal with recoiling daughters? Pharmaceuticals (Basel). 2015;8(2):321–36. https://doi.org/10.3390/ph8020321. Published online 2015 Jun 10.
39. Bhaskar R, Lee KA, Yeo R, Yeoh K-W. Cancer and radiation therapy: current advances and future directions. Int J Med Sci. 2012;9(3):193–9.
40. Murshed H. Radiation biology. In: Fundamentals of radiation oncology. 3rd ed. New York: Academic; 2019. p. 57–87.
41. Sinclair DW. Relative biological effectiveness (RBE), quality factor (Q) and radiation weighting factor (Wr). Ann ICRP. 2003;33(4):1–117.
42. Knapp FF, Dash A, editors. Radiopharmaceuticals for therapy. New Delhi: Springer-India; 2016.
43. Sia J, Szmyd R, Hau E, Gee HE. Molecular mechanisms of radiation-induced cancer cell death: a primer. Front Cell Dev Biol. 2020;8(41):1–8.
44. Desouky O, Ding N, Zhou G. Targeted and non-targeted effects of ionizing radiation. J Radiat Res Appl Sci. 2015;8:247–54.
45. Desouky O, Din N, Zhou G. Targeted and non-targeted effects of ionizing radiation. JRRAS March. 2015;1–8.
46. Panganiban R-AM, Snow AL, Day RM. Mechanisms of radiation toxicity in transformed and non-transformed cells. Int J Mol Sci. 2013;14:15931–58. https://doi.org/10.3390/ijms140815931.
47. Rösch F, Herzog H, Qaim SM. The beginning and development of the theranostic approach in nuclear medicine, as exemplified by the radionuclide pair ^{86}Y and ^{90}Y. Pharmaceuticals. 2017;10:56. https://doi.org/10.3390/ph10020056.
48. Qaim SM, Scholten B, Neumaier B. New developments in the production of theranostic pairs of radionuclides. J Radioanal Nucl Chem. 2018;318:1493–509.
49. Boros E, Packard AB. Radioactive transition metals for imaging and therapy. Chem Rev. 2019;119(2):870–901.
50. Kostelnik TI, Orvig C. Radioactive main group and rare earth metals for imaging and therapy. Chem Rev. 2019;119(2):902–56.

51. Nelson BJB, Andersson JD, Wuest F. Targeted alpha therapy: progress in radionuclide production, radiochemistry, and applications. Pharmaceutics. 2021;13:49. https://doi.org/10.3390/pharmaceutics13010049.
52. Price EW, Orvig C. Matching chelators to radiometals for radiopharmaceuticals. Chem Soc Rev. 2014;43(1):260–90.
53. PI-NaI-2012. Sodium iodide I 131 solution therapeutic for oral use. Package insert. Mallinckrodt, revised 01/2012.
54. PI-Metastron-2013. METASTRON™ (Strontium-89 chloride injection). Package insert. New York: GE Health Care; 2013.
55. Sartor O, Coleman R, Nilsson S, et al. Effect of radium-223 dichloride on symptomatic skeletal events in patients with castration-resistant prostate cancer and bone metastases: results from a phase 3, double-blind, randomized trial. Lancet Oncol. 2014;15(7):738–46.
56. Parker CC, Coleman RE, Sartor O, et al. Three-year Safety of Radium-223 Dichloride in Patients with Castrationresistant Prostate Cancer and Symptomatic Bone Metastases from Phase 3 Randomized Alpharadin in Symptomatic Prostate Cancer Trial. Eur Urol. 2018; 73:427.
57. PI-Quadramet-2018. Quadramet® (Samarium Sm 153 lexidronam injection). Package insert. North Billerica: Lantheus Medical Imaging Inc.; 2018.
58. Braat AJAT, Smits MLJ, Braat MNGJA, et al. ^{90}Y hepatic radioembolization: an update on current practice and recent developments. J Nucl Med. 2015;56:1079–108.
59. Beierwalters WH. Horizons in radionuclide therapy: 1985 update. J Nucl Med. 1981;26:421–6.
60. Bařinka C, Rojas C, Slusher B, Pomper M. Glutamate carboxypeptidase II in diagnosis and treatment of neurologic disorders and prostate cancer. Curr Med Chem. 2012;19:856.
61. Wieland DM, Wu J, Brown LE, Mangner TJ, et al. Radiolabeled adrenergic neuron blocking agents: adrenomedullary imaging with 131I-iodobenzylguanidine. J Nucl Med. 1980;21:349–53.
62. Agrawal A, Rangarajan V, Shah S, et al. MIBG (metaiodobenzylguanidine) theranostics in pediatric and adult malignancies. Br J Radiol. 2018;91:1091.
63. Vallabhajosula S, Nikolopoulou A. Radioiodinated metaiodobenzylguanidine (MIBG): radiochemistry, biology, and pharmacology. Semin Nucl Med. 2011;41:324–33.
64. PI-MIBG-2018. AZEDRA® (iobenguane I 131) injection, for intravenous use. Package Insert. New York, NY: Progenics Pharmaceuticals Inc, revised 07/2018.
65. Hoppenz P, Els-Heindl S, Beck-Sickinger AG. Peptide-drug conjugates and their targets in advanced cancer therapies. Front Chem. 2020;8:571.
66. Reubi J-C. Peptide receptors as molecular targets for cancer diagnosis and therapy. Endocr Rev. 2003;24:389–427. https://doi.org/10.1210/er.2002-0007.
67. Vrettos EI, Mezo G, Tzakos AG. On the design principles of peptide-drug conjugates for targeted drug delivery to the malignant tumor site. Beilstein J Org Chem. 2018;14:930–54. https://doi.org/10.3762/bjoc.14.80.
68. Otte A, Mueller-Brand J, Dellas S, et al. Yttrium-90-labelled somatostatin-analogue for cancer treatment. Lancet. 1998;351(9100):417–8.
69. PI-Lutathera-2018. LUTATHERA® (lutetium Lu 177 dotatate) injection. Package insert. Millburn: Advanced Accelerator Applications; 2018.
70. Köhler G, Milstein C. Continuous cultures of fused cells secreting antibody of predefined specificity. Nature. 1975;256:495–7.
71. Zahavi D, Weiner L. Monoclonal antibodies in cancer therapy. Antibodies. 2020;9(34). https://doi.org/10.3390/antib9030034.
72. Boswell CA, Brechbiel MW. Development of radioimmunotherapeutic and diagnostic antibodies: an inside-out view. Nucl Med Biol. 2007;34:757–78.
73. Larson SM, Carrasquillo JA, Cheung N-KV, Press OW. Radioimmunotherapy of human tumours. Nat Rev Cancer. 2015;15:347–60.
74. O'Keefe DS, Su SL, Bacich DJ, et al. Mapping, genomic organization and promoter analysis of the human prostate-specific membrane antigen gene. Biochim Biophys Acta. 1998;1443:113–27.
75. Horoszewicz JS, Kawinski E, Murphy GP. Monoclonal antibodies to a new antigenic marker in epithelial prostatic cells and serum of prostatic cancer patients. Anticancer Res. 1987;7:927–35.
76. Israeli RS, Powell CT, Corr JG, Fair WR, Heston WD. Expression of the prostate-specific membrane antigen. Cancer Res. 1994;54:1807–11.
77. Liu H, Moy P, Kim S, et al. Monoclonal antibodies to the extracellular domain of prostate-specific membrane antigen also react with tumor vascular endothelium. Cancer Res. 1997;57:3629–34.
78. Liu H, Rajasekaran AK, Moy P, et al. Constitutive and antibody-induced internalization of prostate-specific membrane antigen. Cancer Res. 1998;58:4055–60.
79. Tagawa ST, Akhtar NH, Nikolopoulou A, et al. Bone marrow recovery and subsequent chemotherapy following radiolabeled anti-prostate-specific membrane antigen monoclonal antibody J591 in men with mCRPC. Front Oncol. 2013;3:1–6.
80. Tagawa ST, Sun M, Sartor AO, et al. Phase I study of ^{225}Ac-J591 for men with metastatic castration-resistant prostate cancer (mCRPC). J Clin Oncol. 2021;39(Suppl 15):5015.
81. Vallabhajosula S, Nikolopoulou A, Jhanwar YS, et al. Radioimmunotherapy of metastatic prostate cancer with ^{177}Lu-DOTA-huJ591 anti prostate specific membrane antigen specific monoclonal antibody. Curr Radiopharm. 2016;9:44–53.
82. Pastorino S, Riondato M, Uccelli L, et al. Toward the discovery and development of PSMA targeted

inhibitors for nuclear medicine applications. Current Radiopharmaceuticals. 2020;13:63–79.
83. Carlucci G, Ippisch R, Slavik R, et al. ^{68}Ga-PSMA-11 NDA approval: a novel and successful academic partnership. J Nucl Med. 2021;62:149–55.
84. Morris MJ, Rowe SP, Gorin MA, et al. Diagnostic performance of ^{18} F-DCFPyL-PET/CT in men with biochemically recurrent prostate cancer: results from the CONDOR phase III, multicenter study. Clin Cancer Res. 2021;27(13):3674–82.
85. Weineisen M, Schottelius M, Simecek J, et al. ^{68}Ga- and ^{177}Lu-labeled PSMA I&T: optimization of a PSMA-targeted theranostic concept and first proof-of-concept human studies. J Nucl Med. 2015;56:1169–1176
86. Benešová M, Schäfer M, Bauder-Wüst U, et al. Preclinical evaluation of a tailor-made DOTA-conjugated PSMA inhibitor with optimized linker moiety for imaging and endoradiotherapy of prostate cancer. J Nucl Med. 2015;56(6):914–20.
87. Kratochwil C, Giesel FL, Stefanova M, et al. PSMA-targeted radionuclide therapy of metastatic castration-resistant prostate cancer with ^{177}Lu-labeled PSMA-617. J Nucl Med. 2016;57:1170–6.
88. Hofman MS, Emmett L, Sandhu S, et al. [^{177}Lu] Lu-PSMA-617 versus cabazitaxel in patients with metastatic castration-resistant prostate cancer (TheraP): a randomized, open-label, phase 2 trial. Lancet. 2021;397(10276):797–804.
89. Sartor O, de Bono J, Chi KN, Fizazi K, Herrmann K, Rahbar K, et al. Lutetium-177-PSMA-617 for metastatic castration-resistant prostate cancer. N Engl J Med. 2021;385:1091–103.